β- and γ-spectroscopy study of ^{119}Pd and ^{119}Ag

J. Kurpeta,[1] A. Abramuk,[1] T. Rząca-Urban,[1] W. Urban,[1] L. Canete,[2] T. Eronen,[3] S. Geldhof,[4] M. Gierlik,[5] J. P. Greene,[6] A. Jokinen,[3] A. Kankainen,[3] I. D. Moore,[3] D. A. Nesterenko,[3] H. Penttilä,[3] I. Pohjalainen,[7] M. Reponen,[3] S. Rinta-Antila,[3] A. de Roubin,[8] G. S. Simpson,[9] A. G. Smith,[10] and M. Vilén[11]

[1]*Faculty of Physics, University of Warsaw, ul. Pasteura 5, PL-02-093 Warsaw, Poland*
[2]*Department of Physics, University of Surrey, Guildford, Surrey GU2 7XH, England, United Kingdom*
[3]*Department of Physics, University of Jyväskylä, P.O. Box 35, FIN-40014 Jyväskylä, Finland*
[4]*Instituut voor Kern-en Stralingsfysica, KU Leuven, Leuven, Belgium*
[5]*National Centre for Nuclear Research, ul. Andrzeja Sołtana 7, 05-400 Otwock, Świerk, Poland*
[6]*Argonne National Laboratory, Argonne, Illinois 60439, USA*
[7]*GSI Helmholtzzentrum für Schwerionenforschung GmbH, Darmstadt, Germany*
[8]*Centre National de la Recherche Scientifique IN2P3, Université de Bordeaux, Centre d'Etudes Nucléaires de Bordeaux Gradignan, Gradignan Cedex, France*
[9]*LPSC, Université Joseph Fourier Grenoble 1, Centre National de la Recherche Scientifique IN2P3, Institut National Polytechnique de Grenoble, F-38026 Grenoble Cedex, France*
[10]*Department of Physics and Astronomy, The University of Manchester, M13 9PL Manchester, England, United Kingdom*
[11]*Experimental Physics Department, CERN, CH-1211 Geneva 23, Switzerland*

(Received 21 December 2021; accepted 25 February 2022; published 14 March 2022)

Neutron-rich ^{119}Pd nuclei were produced in fission of natural uranium, induced by 25-MeV protons. Fission fragments swiftly extracted with the Ion Guide Isotope Separation On-Line method were mass separated using a dipole magnet and a Penning trap, providing mono-isotopic samples of ^{119}Pd. Their β^- decay was measured with $\gamma\gamma$- and $\beta\gamma$-spectroscopy methods using low-energy germanium detectors and a thin plastic scintillator. Two distinct nuclear-level structures were observed in ^{119}Ag, based on the $1/2^-$ and $7/2^+$ isomers reported previously. The β^--decay work was complemented by a prompt-γ study of levels in ^{119}Ag populated in spontaneous fission of ^{252}Cf, performed using the Gammasphere array of germanium detectors. Contrary to previous suggestions, our data show that the $1/2^-$ isomer is located below the $7/2^+$ isomer and is proposed as a new ground state of ^{119}Ag with the $7/2^+$ isomer excitation energy determined to be 33.4 keV. Our data indicate that there are two β unstable isomers in ^{119}Pd, a proposed ground state of ^{119}Pd with tentative spin $1/2^+$ or $3/2^+$ and a half-life of 0.88 s and the other one about 350 keV above, having spin $(11/2^-)$ and a half-life of 0.85 s. The higher-energy isomer probably decays to the $1/2^+$ or $3/2^+$ ground state via a γ cascade comprising 18.7-219.8-X-keV transitions. The unobserved isomeric transition with energy $X \approx 100$ keV probably has an $E3$ multipolarity. Its hindrance factor is significantly lower than for analogous $E3$ isomeric transitions in lighter Pd isotopes, suggesting an oblate deformation of levels in ^{119}Pd. Oblate configurations in ^{119}Ag are discussed also.

DOI: 10.1103/PhysRevC.105.034316

I. INTRODUCTION

It is commonly accepted that the prolate type of quadrupole deformation dominates in nuclei [1]. The oblate shape is a much rarer phenomenon on the nuclear chart. Searching for this effect is thus of prime importance for better understanding of nuclear structure.

The prolate shape sets in above closed shells when the number of valence nucleons occupying low-Ω orbitals of the intruder shell is sufficiently large to induce the deformation (see, e.g., Ref. [2]). With the Fermi level approaching high-Ω orbitals the nucleus undergoes a change towards an oblate shape, usually via an intermediate phase of triaxiality.

Above the $Z = 50$ proton shell closure this effect appears when the $i_{13/2}$ proton intruder is nearly filled and was found in osmium, mercury, and platinum isotopes. These observations were facilitated by the fact that the nuclei in question are close to the stability line and therefore easy to access.

Oblate shapes are also expected in other regions of the nuclear chart, where the high-Ω orbitals of intruder shells are active. Within the $28 \leqslant Z \leqslant 50$ major shell the $g_{9/2}$ proton intruder has its high-Ω orbitals active around $Z = 46$. However, the high-Ω orbitals of the $h_{11/2}$ neutron intruder are being filled only in neutron-rich isotopes. This makes the study of the oblate deformation in this region more challenging, however the contemporary high-resolution experimental techniques involving large arrays of γ-ray detectors and precise mass separation render such studies possible.

Neutron-rich nuclei of the mass $A \approx 110$ region can be populated in fission of heavy nuclei and their decays studied

using large arrays of Ge detectors or, more individually, after mass separation. Both techniques were used to trace transitions towards an oblate shape in ^{110}Mo and ^{111}Tc utilizing either the EUROGAM2 array for triple-γ study [3,4] or the Penning-trap separation technique [5]. The effect was also searched for using the Penning-trap technique at $A = 113$ [6], 115 [7], and 117 [8].

Our recent study of ^{107}Mo either populated in β^- decay of isotopically separated ^{107}Nb [9] or deexcited by prompt-γ rays following fission [10] has shown that in cases where there is a sufficient overlap between levels accessed by both techniques one can obtain rich complementary information.

As discussed in Ref. [8], in odd-N palladium isotopes there are $11/2^-$ isomers corresponding to the $h_{11/2}$ neutron, which in their β^- decay may populate yrast levels in silver daughter nuclei. Such levels should also be accessible in measurements of prompt-γ rays following fission of ^{252}Cf, which populates neutron-rich isotopes in this region. In the present paper we report on the study of the neutron-rich ^{119}Ag nucleus, combining both techniques discussed above with the aim to extend our knowledge on the development of oblate deformation in the region.

II. EXPERIMENTS AND RESULTS

A. β decay of ^{119}Pd to ^{119}Ag

The β decay of the neutron-rich ^{119}Pd was first observed at the Ion Guide Isotope Separator On-Line (IGISOL) [11]. In that study five new γ lines 69.9, 129.9, 256.6, 326.1, and 507.2 keV were ascribed to the β decay of ^{119}Pd (the 507.2 keV was not placed in the decay scheme) and the half-life for ^{119}Pd was estimated to be 0.92 ± 0.13 s. A similar half-life value of 0.918 ± 0.111 s was reported in Ref. [12] where ^{119}Pd was produced in fragmentation of a ^{136}Xe primary beam impinging onto a Be target.

In the first study of ^{119}Pd, with the IGISOL mass separator [11], the β-gated low-energy γ spectrum was dominated by the 102.6-keV peak from β decay of ^{103}Nb [13]. The ^{103}Nb and ^{103}Mo isobaric impurities were getting through the IGISOL separator as singly ionized complexes containing ^{16}O. This has been improved in the present paper—the contaminating γ lines of $A = 103$ isobars are not present in the spectra thanks to the use of an ion trap.

1. Experimental techniques

Our study was carried out at the IGISOL facility, recommissioned as IGISOL-4 [14]. Fission of a natural uranium target was induced by 25-MeV protons from the K-130 cyclotron at the Accelerator Laboratory of the University of Jyväskylä. Fission fragments, escaping from the thin target, were slowed down in a He-filled chamber of the IGISOL ion source. The fragments reset to the 1^+ charge state and were evacuated from the chamber with flowing helium. Then a system of electrodes, a sextupole ion beam guide SPIG [15], facilitated their transport to a dipole magnet. The singly ionized fragments of the wanted mass number $A = 119$ were separated with a magnetic field and formed into bunches in a radio-frequency cooler and buncher [16].

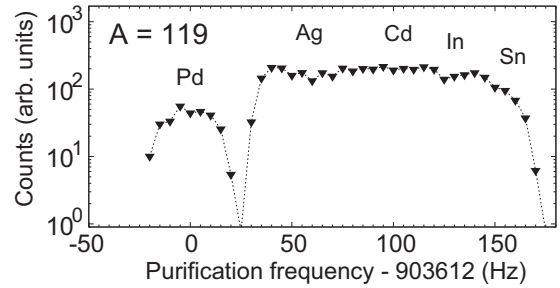

FIG. 1. Ion counts registered with a MCP detector, placed after the Penning trap, as a function of the frequency of the quadrupole radio-frequency field in the purification trap. The resolved atomic ions from the IGISOL isobaric beam are marked with their element symbols.

In the present paper the IGISOL technique was complemented with a Penning trap serving as a very precise mass separator. The side-band cooling technique [17,18] was applied in the purification ion trap, of the JYFLTRAP Penning trap [19], to get rid of the unwanted, less exotic isobars. The JYFLTRAP system consists of two Penning traps located in a 7 T superconducting magnet. For isobaric purification only one of the traps was used while the other was operated in a shoot-through mode.

Figure 1 presents the 1^+ ions of the $A = 119$ mass chain detected with a microchannel plate (MCP) detector located outside the strong magnetic field housing the Penning traps. The quadrupole radio-frequency field was scanned over a wide range of frequencies, to find its resonance frequency value for selecting the palladium ions. The mass resolving power ($R = M/\Delta M$) of the purification trap, based on Fig. 1, can be estimated as 28 000 and the rate of ^{119}Pd$^+$ ions was about 134 s^{-1} assuming efficiency of 28% for the MCP.

The mono-isotopic samples of ^{119}Pd, delivered from the trap, were implanted onto a movable, collection tape surrounded by a 2-mm-thick plastic scintillator. The latter was employed to detect electrons emitted in β^- decay. The implantation point and scintillation detector were located in a vacuum chamber equipped with three windows made of Kapton foil to ensure transmittance of low-energy γ rays. Low-energy Ge (LEGe) detectors were placed around the chamber in close geometry to efficiently register γ radiation. These were the broad-energy germanium detectors of high-energy resolution (full width at half maximum of $\approx$0.5 keV at 20 keV). Three LEGe detectors were placed in a horizontal plane at right angles, each facing a window in the vacuum chamber. The fourth LEGe detector was placed vertically over the chamber. Our detection setup is sketched in Fig. 2.

The total purification cycle of the Penning trap was 111 ms and the ^{119}Pd ions were delivered in a pulsed-beam mode to enable measurement of β-decay half-lives. Two different time patterns were used. In the first time pattern, the mono-isotopic samples of ^{119}Pd were implanted for 1.9 s (the implantation period) and then the beam was blocked for 1.6 s (decay period) and finally the collection tape was moved away to remove the long-lived decay products, and a new cycle started. In the second pattern, the samples were implanted for 6 s, the beam

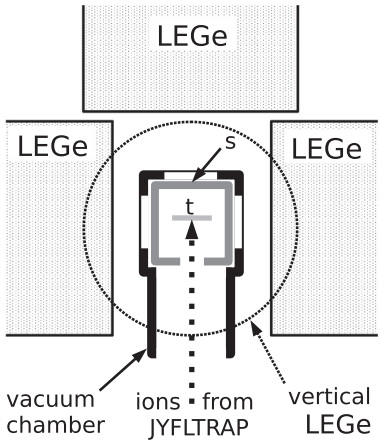

FIG. 2. Horizontal section of the detection setup. Bunches of mono-isotopic ions from the trap are implanted into a movable tape (t). Electrons are detected by a thin plastic scintillator (s), mounted inside a metal vacuum chamber. Low-energy γ rays are transmitted by the Kapton windows located in the horizontal plane. The LEGe detectors are arranged closely around the vacuum chamber; the position of the vertical one is marked with a dotted line.

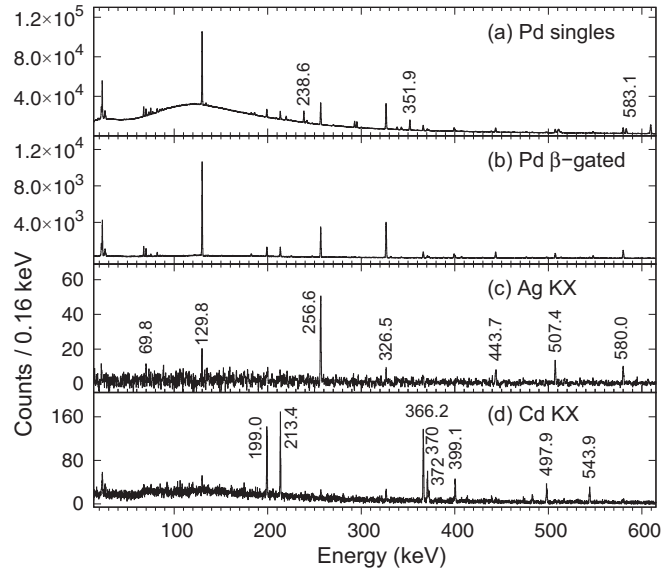

FIG. 3. The singles (a), β-gated (b), and x-ray-gated spectra measured with the LEGe detectors for the mono-isotopic samples of ^{119}Pd. The spectra in the panels (c) and (d) are gated by the sum of K_α and K_β x rays of silver and cadmium, respectively. The peaks are labeled with their energies in keV.

was blocked for 2 s, and then the collection tape was moved away, and a consecutive cycle started.

The data acquisition system using the digital gamma finder modules of digital pulse processors was recording signals from all the detectors in a triggerless mode. Later off line, collected data were time ordered and sorted into one- and two-dimensional histograms for further analysis.

2. *Identification of γ transitions*

The γ spectra following β decay of mono-isotopic samples of ^{119}Pd are shown in Fig. 3. The singles spectrum shown in Fig. 3(a) contains all events registered in the germanium detectors with no gating conditions. One can observe the strongest γ lines populated in the β decay of ^{119}Pd as well as lines from natural background of γ radiation, seen at 238.6, 351.9, and 583.1 keV. At low energies there is a pronounced, continuous background due to the Compton scattering.

Figure 3(b) shows a spectrum of events measured by γ detectors, which are in coincidence with any β particle registered in the plastic scintillation counter. Demanding a coincidence with β particles suppresses all γ events which do not occur immediately after β decay. Thus the spectrum in Fig. 3(b) presents γ and x rays directly related to the β decay of ^{119}Pd and its daughter nuclei.

The spectra in Figs. 3(c) and 3(d) are gated by x-ray lines corresponding to silver and cadmium atoms, respectively. The coincidence of γ lines with silver x rays, shown in the spectrum in Fig. 3(c), identifies them as populated in the decay of their palladium parent. In the same way, the spectrum in Fig. 3(d) presents γ lines populated in the β decay of silver. The Penning trap delivers mono-isotopic samples of ^{119}Pd. Therefore, γ spectra seen in Figs. 3(c) and 3(d) show transitions in ^{119}Ag and ^{119}Cd, respectively.

The spectrum shown in Fig. 3(c) confirms that the 69.9-, 129.9-, 256.6-, 326.1-, and 507.2-keV lines reported in Ref. [11] belong to the ^{119}Pd decay and shows new γ lines observed for the first time in this paper. The γ lines in coincidence with cadmium K x rays, shown in Fig. 3(d), are in accordance with the previous results on the β^- decay of ^{119}Ag [20]. The consecutive β decays in the $A = 119$ chain, namely, ^{119}Cd to ^{119}In and ^{119}In to ^{119}Sn (stable), are considerably suppressed by the collection-tape cycle, because of their half-lives for the ground and isomeric states, which are longer than 2 min.

3. *β-decay scheme of* ^{119}Pd

The coincidence γ-ray spectra for mono-isotopic samples of ^{119}Pd were made by setting gates on two-dimensional histograms. The examples of our coincidence spectra are presented in Fig. 4. Analysis of such gated spectra provided coincidence relations between γ transitions populated in the β^- decay of ^{119}Pd. The obtained coincidence relations are shown in Table I.

Energies and relative intensities of γ lines were determined based on singles spectra, such as the one shown in Fig. 3(a). For a few weak γ lines the intensities were adopted from a β-gated spectrum or estimated on the basis of coincidence spectra. In several cases of doubly placed γ lines or belonging to more than one isotope, the intensities were divided with coincidence relations, too.

The coincidence relations and intensities of γ lines from Table I were used to construct the β-decay scheme of ^{119}Pd shown in Fig. 5. In total 33 new excited levels were observed in ^{119}Ag in the present β-decay measurement.

We found that excited levels in ^{119}Ag form two distinct structures, shown as "bands" A and B in the decay scheme in Fig. 5. In the bands A and B, there are several transitions

TABLE I. Energies, relative intensities I_γ, placement in the scheme, and coincidence relations observed in the β^- decay of ^{119}Pd. The energy 22.1 keV is the K_α silver characteristic x rays.

E_γ(keV)	I_γ	From	To	Coincident γ lines (keV)
22.1(2)				129.8 256.6 326.5 443.7 507.4 547.9 580.0 689.8 831.4
69.8(2)	7.3 (0.4)	326.5	256.6	22.1 256.6 443.7 (534.0) (547.9) 580.0 (684.3)
136.2(2)	0.9 (0.2)	906.4	770.2	256.6 326.5 443.7 (580.0)
256.6(2)	62.0 (3.1)	256.6	0.0	22.1 69.8 429.7 443.7 513.4 547.9 580.0 617.6 (684.3) (756.8) 775.3 831.4 1010.2 1035.7 (1102.1)
282.6(2)	1.1 (0.2)	1440.5	1157.8	(69.8) (256.6) (831.4)
326.5(1)	99.1 (5.0)	326.5	0.0	(136.2) 282.6 (359.8) (387.9) 443.7 534.0 547.9 580.0 672.6 684.3 705.5 756.8 831.4 (897.4) 904.7 (919.0) (982.3)
359.8(2)	1.2 (0.2)	686.2	326.5	326.5
387.9(2)	2.3 (0.2)	1157.8	770.2	256.6 326.5 443.7
429.7(2)	2.4 (0.2)	686.2	256.6	256.6
443.7(1)	24.5 (1.2)	770.2	326.5	22.1 69.8 (136.2) 256.6 326.5 387.9 670.4 684.3 (919.0)
513.4(2)	8.4 (0.7)	770.2	256.6	256.6
534.0(2)	4.5 (0.3)	1440.5	906.4	69.8 256.6 326.5 580.0
547.9(1)	13.2 (0.7)	1454.4	906.4	22.1 69.8 256.6 326.5 580.0
580.0(1)	48.8 (2.5)	906.4	326.5	22.1 69.8 256.6 326.5 534.0 547.9 672.6 756.8 (897.4) 904.7 (982.3)
607.3(2)[a]	1.0 (0.5)	1481.5	874.4	(256.6) (326.5) (617.6)
617.6(2)[b]	9.1 (0.6)	874.4	256.6	256.6 (607.3)
670.4(2)	3.5 (0.3)	1440.5	770.2	(69.8) 256.6 326.5 443.7
672.6(2)	4.0 (0.3)	1579.0	906.4	(256.6) 326.5 580.0
684.3(2)	2.9 (0.3)	1454.4	770.2	(22.1) 69.8 256.6 326.5 443.7
686.2(1)	8.9 (0.5)	686.2	0.0	
705.5(3)[a]	1.1 (0.4)	1032.1	326.5	(69.8) 256.6 326.5
756.8(2)	5.7 (0.4)	1663.2	906.4	69.8 256.6 326.5 580.0
775.3(2)	2.1 (0.3)	1032.1	256.6	256.6 326.5
831.4(2)	13.1 (0.7)	1157.8	326.5	(22.1) 69.8 256.6 282.6 326.5
874.7(3)	1.9 (0.4)	874.4	0.0	
897.4(2)	3.2 (0.3)	1803.7	906.4	256.6 326.5 580.0
904.7(2)	3.1 (0.5)	1811.1	906.4	326.5 (580.0)
919.0(3)	1.9 (0.3)	1689.0	770.2	(256.6) (326.5) (443.7)
982.3(2)	2.9 (0.3)	1888.5	906.4	256.6 326.5 580.0
1010.2(2)	3.1 (0.4)	1266.8	256.6	256.6
1032.2(2)	4.3 (0.4)	1032.1	0.0	
1035.7(3)	1.6 (0.3)	1291.9	256.6	256.6
1102.1(2)[c]	4.2 (0.5)	1358.6	256.6	
1157.0(4)	1.3 (0.4)	1157.8	0.0	
1291.6(3)	2.1 (0.3)	1291.9	0.0	
1358.3(4)	1.7 (0.4)	1358.6	0.0	
1688.9(4)	1.9 (0.5)	1689.0	0.0	
1887.9(4)	1.7 (0.3)	1888.5	0.0	
129.8(1)	100.0 (5.1)	163.2	33.4	182.4 507.4 536.6 550.7 607.3 689.8 705.5 725.8 950.5 987.8 1006.9 1038.9 (1118.0) 1213.5 (1686.2) 1950.7 1998.5 2100.8 (2254.6) (2655.2)
182.4(2)	2.9 (0.2)	853.0	670.6	129.8 507.4 725.8 950.5
456.6(2)	1.6 (0.2)	1170.3	713.9	680.5
507.4(1)	26.3 (1.4)	670.6	163.2	22.1 129.8 182.4 536.6 (705.5) (725.8) 1038.9
536.6(2)	2.1 (0.3)	1207.2	670.6	129.8 507.4
550.7(2)	2.4 (0.3)	713.9	163.2	129.8
607.3(2)[a]	3.5 (0.5)	770.2	163.2	129.8
680.5(1)	14.1 (0.8)	713.9	33.4	456.6
689.8(1)	9.8 (0.6)	853.0	163.2	22.1 129.8 725.8 950.5
705.5(2)[a]	2.0 (0.3)	1376.6	670.6	129.8 507.4
725.8(2)	2.4 (0.3)	1579.0	853.0	129.8 182.4 (507.4) 689.8
950.5(2)	6.8 (0.5)	1803.7	853.0	129.8 182.4 (507.4) 689.8
987.8(2)	2.8 (0.3)	1151.0	163.2	129.8
1006.9(2)	3.6 (0.3)	1170.3	163.2	129.8
1038.9(3)	1.5 (0.4)	1709.5	670.6	129.8 507.4

TABLE I. (*Continued.*)

E_γ(keV)	I_γ	From	To	Coincident γ lines (keV)
1118.0(5)	1.9 (0.4)	1281.2	163.2	129.8
1213.5(2)	5.1 (0.6)	1376.6	163.2	129.8
1343.5(3)	2.2 (0.4)	1376.6	33.4	
1686.2(5)	1.2 (0.4)	1849.4	163.2	129.8
1950.7(4)	3.3 (0.3)	2113.9	163.2	129.8
1998.5(5)	1.9 (0.3)	2161.8	163.2	129.8
2100.8(5)	4.1 (0.4)	2264.0	163.2	129.8
2128.5(5)	1.9 (0.3)	2161.8	33.4	
2254.6(7)	3.3 (0.5)	2417.8	163.2	129.8
2655.2(10)	3.3 (0.3)	2818.4	163.2	129.8

[a]Doubly placed.
[b]Intensity in coincidence with β.
[c]Also in ^{119}In.

populating the ground state of ^{119}Ag, for which no coincidence relations with other transitions were seen. These lines were placed in the scheme when their energy fitted the difference between the ground state and the energy of the initial level, which was based on at least one coincidence relation. In the band *B*, there are five levels located higher than 2 MeV, which are in coincidence with the 129.8-keV transition (for the compactness of Fig. 5 the positions of these levels are shown not to scale).

In band *B* there are γ transitions which are similar in energy to the 130.0-, 182.2-, 507.2-, 536.4-, and 689.4-keV transitions in ^{119}Ag seen in the prompt-γ study of ^{252}Cf fission in Ref. [22], which form the same medium-spin structure as reported there. We note that levels of part *A*, partly seen in Ref. [11], were not reported in Ref. [22].

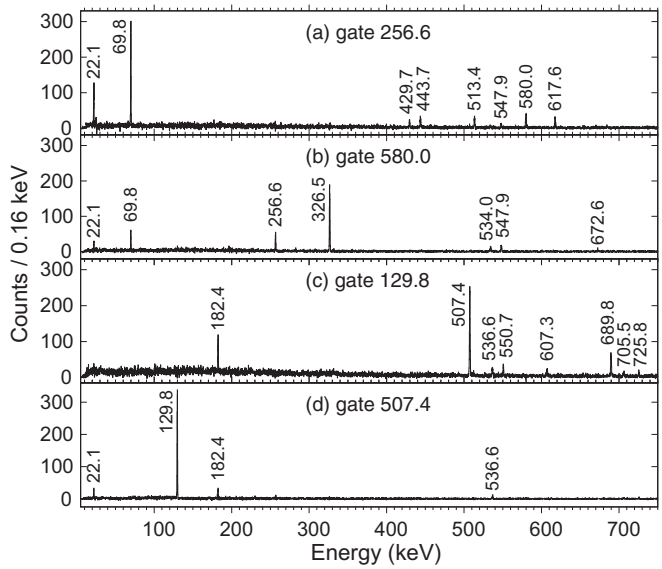

FIG. 4. The coincidence γ spectra for mono-isotopic samples of ^{119}Pd. The spectra (a) and (b) are gated by the 256.6- and 580.0-keV lines, which belong to the band *A*. The spectra (c) and (d) are gated by the 129.8- and 507.4-keV lines, which belong to the band *B*. Bands *A* and *B* are shown in the scheme in Fig. 5. The peaks are labeled with their energies in keV.

The compilation for mass $A = 119$ [23] reports two isomers at low energy in ^{119}Ag, a lower one with tentative spin parity $(7/2^+)$, the half-life of 2.1 s, and unknown excitation energy and the other with tentative spin parity $(1/2^-)$, the half-life of 6.0 s, and unknown energy, located just above the $(7/2^+)$ isomer. The relative positions of the two isomers were probably proposed based on the properties of β^- decay of ^{119}Ag to ^{119}Cd [23], where only the decay of the $(7/2^+)$ isomer in ^{119}Ag is reported, as can be identified by the decay half-life.

An important new observation of the present paper is the possible link between the bands *A* and *B*, which are based on the $1/2^-$ and $7/2^+$ isomers, respectively. Figure 5 shows that when band *B*, based on the $(7/2^+)$ isomer, is placed 33.4 keV above the $(1/2^-)$ isomeric head of band *A* three levels 770.2, 1579.0, and 1803.7 keV turn out to be common for both the bands, thus fixing the so far unknown relative positions of the two isomers in ^{119}Ag. The three levels, together with the 906.4-keV one (linked via the 136.2-keV transition to the 770.2 level), decay to both bands.

This very suggestive observation needs to be confirmed by $\gamma\gamma$ coincidence data because of its important implications. If confirmed, the $1/2^-$ isomer becomes the candidate for the ground state of ^{119}Ag in contrast to the suggestion of the compilation [23]. Furthermore, with the $1/2^-$ isomer below the $7/2^+$ one there should also be β^- decay of the $1/2^-$ isomer to low-spin levels in ^{119}Cd, possibly to the $1/2^+$ ground state and the $3/2^+$ level at 27.0 keV, for which $\log_{10} ft$ are not reported [23].

The 136.2-keV transition from the 906.4-keV to the 770.2-keV level used as a gate in our $\gamma\gamma$ coincidence data shows coincidences with the strong 443.7-keV transition (see Table I) but the 607.3-keV transition is too weak to be seen in this gate. However, the complementary prompt-γ data analyzed in the present paper deliver firm evidence confirming the position of the $7/2^+$ isomer 33.4 keV above the $1/2^-$ isomer, as discussed in detail in Sec. II B.

We note that any hypothetical, low-spin level located below the $1/2^-$ isomer and having spin in a range from 1/2 to 13/2

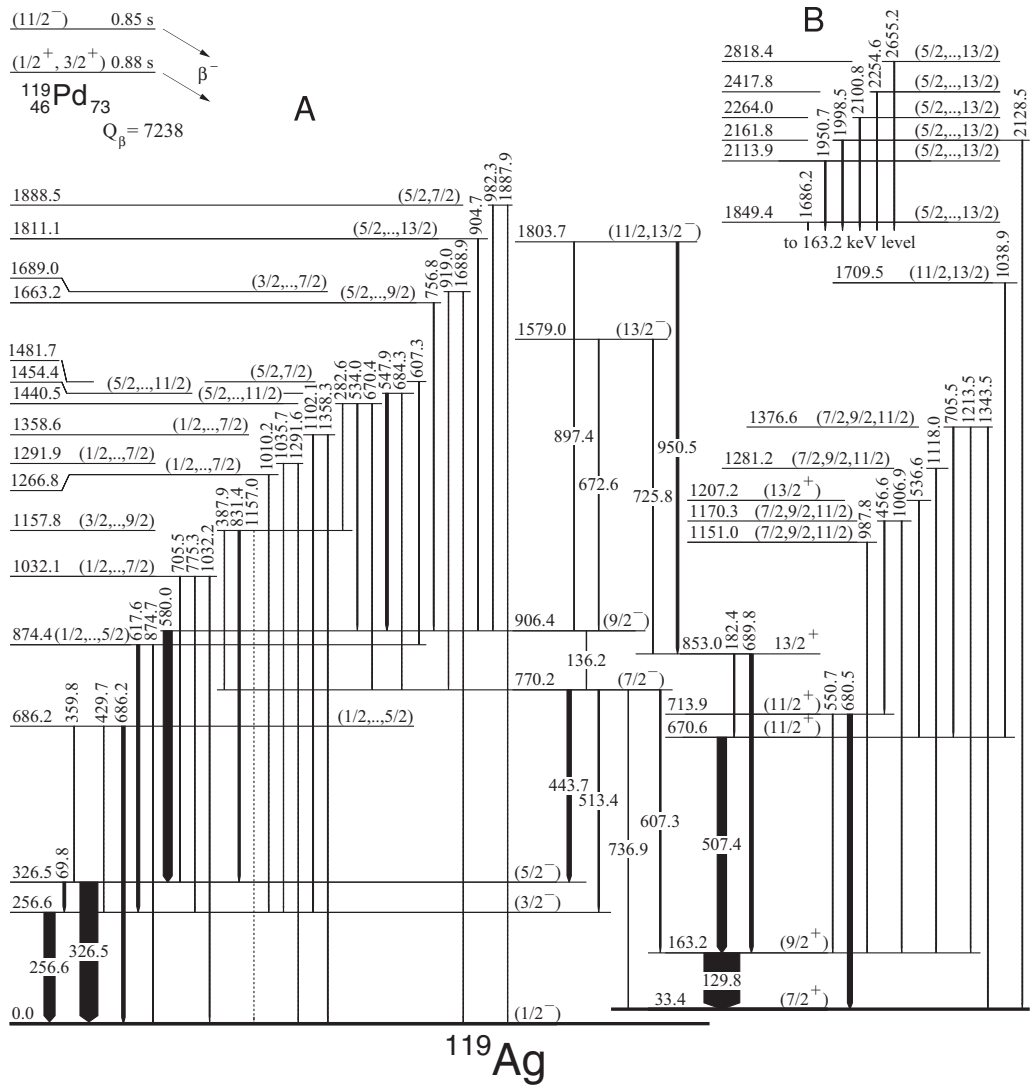

FIG. 5. The scheme of levels in ^{119}Ag fed by β^- decay of ^{119}Pd, obtained in this paper. The half-life values are from this paper and the Q_β value (in keV) is from Ref. [21]. The widths of the arrows are approximately proportional to γ intensities. The energy values are in keV. The two band structures are marked with the capital letters *A* and *B*.

should be populated in the decay of levels of band *A* or *B*. As no such decays are observed, we postulate that the $1/2^-$ isomer is the ground state of ^{119}Ag.

Spin and parity assignments to the levels in ^{119}Ag shown in Fig. 5 are discussed in detail in Sec. II C, after all the data obtained in measurements of β^- decay and prompt γ from fission are presented.

4. Internal conversion and β feedings

To estimate the β feeding intensities to excited levels in ^{119}Ag, one has to use the total intensities of the γ transitions. Thus the intensities of the low-energy γ lines in Table I must be corrected for internal conversion.

Using our data, internal conversion coefficients (ICCs) were determined by comparing the intensity of the transition in question to the intensity of characteristic K x rays of silver in a gated spectrum. In this way we found the α_K ICCs for the 69.8- and 129.8-keV transitions, using the spectra gated by 256.6- and 507.4-keV γ lines [see Figs. 4(a) and 4(d)]. Our results are compared in Table II to theoretical ICC values from Ref. [24].

We confirm the $M1$ multipolarity of the 69.8-keV transition, reported in Ref. [11], where the ICC for the 69.8-keV

TABLE II. The experimental values of internal conversion coefficients and the deduced multipolarities of γ transitions. Theoretical internal conversion coefficients from Ref. [24].

E		α_K^{theor}				
(keV)	α_K^{exp}	$E1$	$M1$	$E2$	Mult.	Ref.
69.9	1.03 ± 0.40	0.384	1.01	3.53	$M1$	[11]
69.8	0.95 ± 0.09				$M1$	This paper
129.8	0.19 ± 0.02	0.066	0.176	0.455	$M1$	This paper

TABLE III. Experimental β feeding intensities (I_β) and $\log_{10} ft$ values of excited levels populated in the β^- decays of the ground and isomeric states in ^{119}Pd. For band B we assumed the $11/2^-$ isomer at 350 keV [see Fig. 15(b)].

Band A			Band B		
E_{lev}(keV)	I_β	$\log_{10} ft$	E_{lev} (keV)	I_β	$\log_{10} ft$
0.0	0.0		33.4(1)	0.0	
256.6(2)	9.5(1.8)	5.92	163.2(2)	34.5(3.9)	5.41
326.5(1)	15.0(2.7)	5.70	670.6(2)	12.6(1.4)	5.72
686.2(1)	6.6(0.4)	5.96	713.9(2)	10.8(1.1)	5.77
770.2(1)	11.2(0.8)	5.70	770.2(1)	2.5(0.4)	6.39
874.4(3)	5.3(0.5)	6.00	853.0(2)	2.7(0.7)	6.33
906.4(1)	7.0(1.4)	5.86	1151.0(3)	2.0(0.3)	6.37
1032.1(2)	4.0(0.4)	6.07	1170.3(2)	3.8(0.4)	6.09
1157.8(3)	8.2(0.5)	5.71	1207.2(3)	1.5(0.3)	6.48
1266.8(3)	1.6(0.2)	6.38	1281.2(5)	1.4(0.3)	6.49
1291.9(3)	2.0(0.2)	6.29	1376.6(2)	6.7(0.8)	5.78
1358.6(2)	3.1(0.4)	6.07	1579.0(1)	1.7(0.3)	6.31
1440.5(2)	4.8(0.3)	5.85	1709.5(4)	1.1(0.3)	6.46
1454.4(2)	8.5(0.5)	5.60	1803.7(2)	4.9(0.5)	5.78
1481.7(3)	0.5(0.3)	6.80	1849.4(5)	0.9(0.3)	6.50
1579.0(1)	2.1(0.2)	6.16	2113.9(5)	2.4(0.3)	5.98
1663.2(2)	3.0(0.2)	5.98	2161.8(4)	2.7(0.4)	5.91
1689.0(3)	2.0(0.3)	6.15	2264.0(5)	3.0(0.4)	5.83
1803.7(2)	1.7(0.2)	6.18	2417.8(7)	2.4(0.4)	5.87
1811.1(2)	1.6(0.3)	6.19	2818.4(10)	2.4(0.3)	5.72
1888.5(4)	2.4(0.2)	5.99			

transition was estimated experimentally to be $\alpha_K = 1.03 \pm 0.40$. The important new result is the $M1$ multipolarity of the 129.8-keV transition.

For the transitions 136.2, 182.4, and 282.6 keV we assumed $M1$, for 256.6 keV we assumed an equal mixture of $M1$ and $E2$, and we assumed $E2$ for 326.5 keV. In all the cases the respective total ICCs were calculated with the BRICC code [24].

In the proposed scenario the transitions from the $(1/2^+, 3/2^+)$ ^{119}Pd ground state to the 33.4-keV $(7/2^+)$ level are of the second forbidden character and β feeding to the 33.4-keV level is completely negligible. The transition from the $(11/2^-)$ isomer in ^{119}Pd to the 33.4 $(7/2^+)$ level is the first forbidden one. Thus it is considerably hindered relative to allowed β transitions. Due to very exotic character (resulting from very low production in fission) of the investigated ^{119}Pd decay, we mainly observe its allowed β transitions. Therefore one can approximately assume no feeding to the 33.4-keV level in β decay.

The β feeding intensities in the decay of ^{119}Pd to the excited levels in ^{119}Ag, as well as the $\log_{10} ft$ values (calculated with an on-line analysis program [25]), are presented in Table III. The strength of β^- feeding to a given level is evaluated as a balance of the γ intensities populating and depopulating the level. Many low-intensity γ lines always escape detection by a spectroscopy setup, so the experimental β feeding intensities should be considered as upper limits, only. Consequently, the $\log_{10} ft$ values represent lower limits.

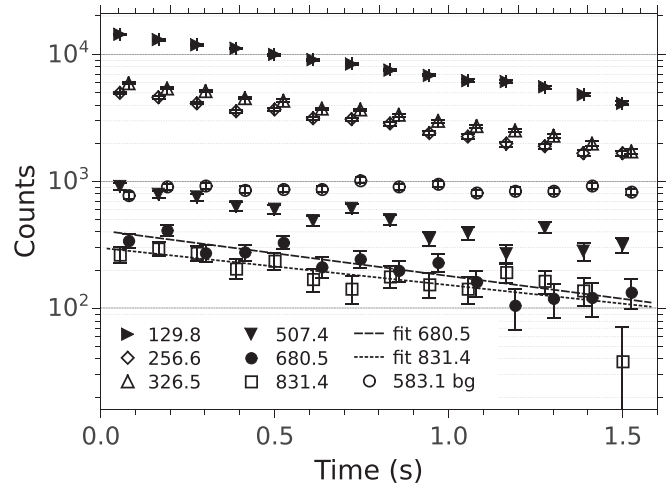

FIG. 6. Time decay pattern for selected γ lines fed in β^- decay of mono-isotopic samples of ^{119}Pd. The fitted exponential-decay curves are shown for γ lines with the shortest (680.5-keV) and the longest (831.4-keV) half-life. Circles mark the 583.1-keV line from the natural γ background. Energies of γ lines in the legend are in keV.

For the 770.2-, 1579.0-, and 1803.7-keV levels, which are common for the bands A and B, their β feedings were estimated separately for each of the bands. The 906.4 -keV level, which is linked to the 770.2-keV level by a weak 136.2-keV transition, was treated as belonging solely to the band A.

5. *Half-lives in the β decay of* ^{119}Pd

We used a decay period of 1.6 s to estimate the half-lives of γ lines populated in the β^- decay of ^{119}Pd. For every γ peak the decay period was divided into 14 equal time bins. In Fig. 6, peak areas for a γ line of a given energy obtained in consecutive time bins are drawn as a function of time. To keep it readable we show the decay patterns for a few selected γ energies, only. The 583.1-keV γ line originates from the natural radiation background and is shown for comparison, as its half-life is much longer than the 1.6-s time base. For each γ line of a sufficient intensity, populated in β decay of ^{119}Pd, an exponential-decay curve was fitted. The resulting half-life values are shown in Table IV.

The half-lives of lines in bands A and B of the β-decay scheme of ^{119}Pd are shown in separate columns in Table IV. The weighted average half-lives are 0.88(2) and 0.85(1) s for bands A and B, respectively, which are the same within one standard deviation and also agree with the 0.86(8)-s half-life of the K_α x-ray radiation of silver, shown in the third column in Table IV. We tentatively assign these half-lives to the respective β-decaying isomers in ^{119}Pd, as shown in Fig. 5.

As discussed in detail in the next section we have identified three new γ transitions with energies of 18.7, 219.8, and 617.6 keV, which are not placed in the excitation scheme of ^{119}Ag. The time-decay patterns of the 219.8- and 617.6-keV lines are shown in Fig. 7 and the resulting half-lives are listed in the last column of Table IV.

TABLE IV. The half-lives of the strongest γ lines and Ag K_α x rays (22.1 keV) populated in β^- decay of ^{119}Pd, from this paper. The uncertainties are purely statistical. Symbol $\overline{T}^{w}_{1/2}$ denotes the weighted-average half-life. The half-lives of the 219.8- and 617.6-keV γ lines in the third column are discussed in Sec. II A 6.

Band *A*		Band *B*		Other lines	
E_γ (keV)	$T_{1/2}$ (s)	E_γ (keV)	$T_{1/2}$ (s)	E_γ (keV)	$T_{1/2}$ (s)
69.8	0.85(7)	129.8	0.849(14)	22.1	0.86(8)
256.6	0.88(3)	507.4	0.86(9)	219.8	0.8(1)
326.5	0.86(2)	680.5	0.84(11)	617.6	3.5(17)
443.7	0.91(6)			617.6	1.3(4)[a]
547.9	0.95(13)				
580.0	0.94(6)				
831.4	1.03(19)				
$\overline{T}^{w}_{1/2}=0.88(2)$		$\overline{T}^{w}_{1/2}=0.85(1)$			

[a]In coincidence with β.

The half-life of the 18.7-keV isomeric transition could not be determined using the above method because of its low intensity. We used another method calculating peak areas in the second time pattern mentioned in Sec. II, where the implantation period of 6 s was followed by a 2-s decay period. The 18.7-keV peak area observed in the implantation period was divided by the area of the same peak observed in the decay period, providing the ratio of 2.4(5). To relate this ratio to the half-life estimate of the 18.7-keV line, we assumed that the activity emitting the 18.7-keV γ rays was delivered directly from the ion trap, and calculated the ratio of growth to decay for various half-lives of this activity. The experimental ratio of 2.4(5) was found to correspond to a half-life of 3.0(6) s. This is a rough estimate because our calculation using an exponential model of decay does not account for background events and we do not know the exact number of the decaying nuclei implanted in each trap cycle.

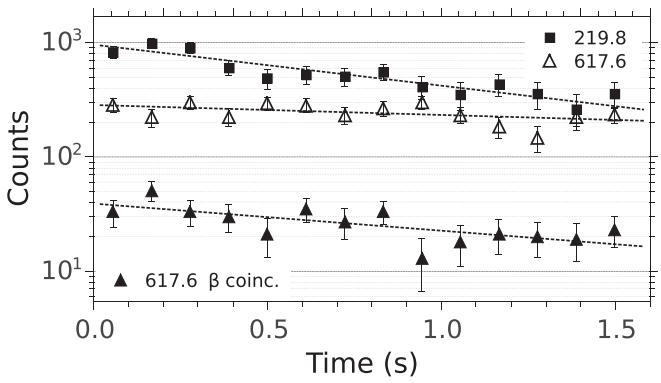

FIG. 7. Time decay pattern for the 219.8- and 617.6-keV γ lines. For the 617.6-keV line its decay is shown in coincidence with β particles too. The fitted exponential decay curves are shown by dashed lines. Energies of γ lines in the legend are given in keV.

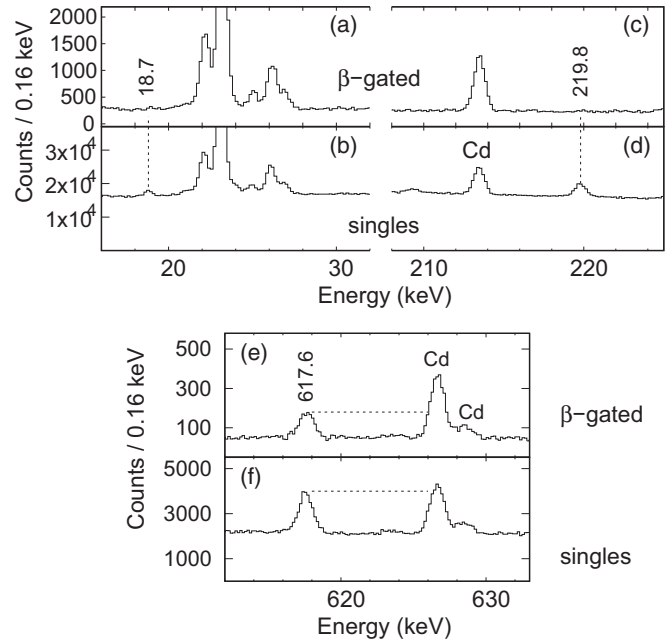

FIG. 8. The singles and β-gated γ spectra for mono-isotopic samples of ^{119}Pd. The three energy ranges contain peaks 18.7, 219.8, and 617.6 keV which are present in the singles spectra (b, d, f) but disappear (a, c) or are considerably reduced (e) in the β-gated spectra. Cd marks γ lines in ^{119}Cd fed in the β decay of ^{119}Ag.

6. *Singles versus β-gated γ spectra: A possible 18-220-keV isomeric cascade in* ^{119}Pd.

Comparison of Figs. 3(a) and 3(b) shows how efficiently various unwanted, background events are removed by gating on β signals. Analogously, the β gating suppresses γ lines depopulating isomeric states. The latter observation helps to search for weakly populated, short isomeric cascades, not easy to spot when using conventional $\gamma\gamma$ techniques.

Figure 8 presents three interesting fragments of our singles and β-gated γ spectra, the comparison of which reveals possible isomeric transitions. Figures 8(a) and 8(b) show the low-energy region for the β-gated and the singles γ spectra below the K x-ray lines of palladium and silver. One notes the 18.7-keV peak in the singles, which is suppressed in the β-gated spectrum. It is helpful to give a quantitative measure of its statistical significance. Here we use the concept of visibility of a peak [26], defined as the ratio of the peak area and the standard deviation of the total number of counts in the region of interest. Visibility of the 18.7-keV peak in Fig. 8(b) is around 16, clearly pointing to its statistical significance.

The low energy of the 18.7-keV transition makes it strongly converted, so in a photon detector we observe only a small fraction of its intensity. The two lowest total ICCs for silver are $\alpha_{\rm tot}(E1,\ 18.7\ {\rm keV}) = \alpha_L + \alpha_M + \cdots = 2.59$ and $\alpha_{\rm tot}(M1,\ 18.7\ {\rm keV}) = 7.39$ (conversion on the K electron shell is forbidden by energy conservation). The total ICCs for any higher multipolarities are at least two orders of magnitude larger. For a palladium isotope the $\alpha_{\rm tot}(E1)$ and $\alpha_{\rm tot}(M1)$ values are lower by about 5 and 10%, respectively, and other total ICCs are again at least two orders of magnitude

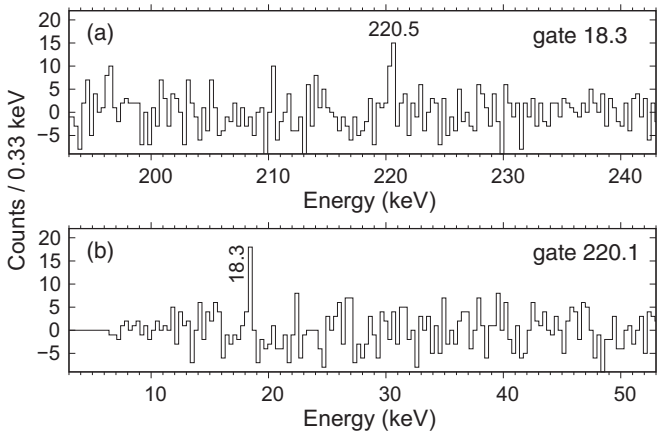

FIG. 9. The spectra in the panels (a) and (b) present the γ events in coincidence with the gates centered at the energies 18.3 and 220.1 keV, respectively. They are close to the energies of the peaks at 18.7 and 219.8 keV, which are related to an unknown isomeric state.

greater. Therefore, the fact that we observe the 18.7-keV line in our spectra suggests its dipole ($l = 1$) character.

In Fig. 8(d) one clearly sees a peak at 219.8 keV, which is not present in the β-gated γ spectrum of Fig. 8(c). The 219.8-keV line cannot be ascribed to any decay scheme in the decay chain of ^{119}Pd. In particular, in the coincidence γ spectrum gated on the 219.8-keV line, there are no peaks in the region of K x rays of silver, palladium, or cadmium. Thus, the 219.8-keV transition is not significantly converted, which suggests its low multipolarity. Therefore, it is rather not a transition directly depopulating an isomeric state. We conclude that the 219.8-keV transition is in a cascade deexciting an isomeric state.

The 18.7(2)- and 219.8(1)-keV lines, seen in singles spectra in Figs. 8(b) and 8(d), respectively, are very interesting because of their possible relation to an unknown isomeric state.

Apparently, the two γ lines show a coincidence relation. Such a coincidence is difficult to measure due to the exotic character of the investigated samples of ^{119}Pd. To observe it we used a two-dimensional histogram, consisting of pairs of γ events registered by the LEGe spectrometers. By varying coincidence gates around the 18.7- and 219.8-keV energies we found the maximum coincidence relation for gating windows centered at 18.3 and 220.1 keV, respectively as shown Fig. 9. In the γ spectrum gated at 18.3 keV, shown in Fig. 9(a), there is a peak at 220.5(4) keV, about 1.7 standard deviations off the 219.8(1)-keV energy. In the γ spectrum gated by 220.1 keV, shown in Fig. 9(b), there is a peak at 18.3(3) keV, shifted by 1.2 sigma relative to the 18.7-keV energy. As the differences are lower than 2 sigma it is possible that the 18.3- and 220.5-keV lines in the coincidence spectra in Fig. 9 are the same as 18.7 and 219.8 keV in Figs. 8(b) and 8(d).

Each of the spectra in Fig. 9 results from subtraction of two spectra, one gated on a peak and the other on the respective background. Due to low counts statistical fluctuations in the spectra are relatively high, as seen in Fig. 9. For both the 18.3- and 220.5-keV peaks, their areas are around 20 counts with uncertainty of about 25%. The peak visibility benchmark is roughly equal to 4 for the 18.3-keV peak and 5 for the 220.5-keV peak.

TABLE V. Properties of the γ lines related to the decay of unknown isomeric states. Energy and intensity in the singles spectrum are given in the first two columns. The third column is the centroid of the window set on the gated line. The column "Mult." shows the proposed multipolarity.

E_γ (keV)	I_γ (rel.)	Gate (keV)	Coincident γ lines (keV)	Mult.
18.7(2)	3.1(3)	18.3	220.5(4)	$l = 1$
219.8(1)	8.9(5)	220.1	18.3(3)	$l \leqslant 2$
617.6(2)	16.7(9)			
617.6(2)	9.1(6)[a]	617.6	In Table I	

[a]In coincidence with β.

The 18-220-keV cascade is not coincident with any other line and is not reported in any known decay scheme of neutron-rich $A = 119$ isobars. Since these lines were neither reported in any of the neutron-rich $A = 119$ isobars [23] nor in the γ-radiation laboratory background recorded during the experiment, we postulate that they form a cascade related to an isomer in ^{119}Pd, populated in fission. The 18-220-keV cascade is similar to the 34.6-97.0-keV cascade in ^{117}Pd populated by the 71.4-keV isomeric transition from the 19-ms isomer [8].

The above observations and the population of two distinctly different bands A and B in ^{119}Ag in β decay of ^{119}Pd strongly suggest that there are two different β-decaying states in ^{119}Pd. Such a possibility was hinted before by the energy-level systematics for odd-A Pd isotopes shown in Figs. 6 and 8 of Ref. [8].

Figures 8(e) and 8(f) show a line at 617.6 keV near the 626.7-keV line from the β^- decay of ^{119}Ag. In the singles γ spectrum, in panel (f), the 617.6- and 626.7-keV lines are of about the same area. In the β-gated spectrum, in panel (e), the area of the 617.6-keV peak is reduced as compared to the 626.7-keV line. Moreover, when observed in coincidence with β particles, the half-life of the 617.6-keV line is 1.3 $\pm$ 0.4 s, which is almost three times shorter than the 3.5 $\pm$ 1.7-s half-life in the singles spectrum (see Table IV). On the other hand, taking into account their large error bars, the two half-lives may overlap. We may hypothesize that the 617.6-keV line consists of two components. One component is in coincidence with β particles and is placed in band A of the ^{119}Pd β-decay scheme. The other component, corresponding to the 3.5-s half-life, cannot be unambiguously ascribed to any of the nuclei in the decay chain of ^{119}Pd.

The 617.6-keV γ line was neither reported in any of the neutron-rich $A = 119$ isobars [23] nor was it found in the laboratory γ-radiation background. It is likely that this transition may also be associated with ^{119}Pd, the most exotic isobar in our data.

The properties of the discussed isomeric lines are collected in Table V.

B. ^{119}Ag populated in spontaneous fission of ^{252}Cf

Medium-spin, yrast, and near-yrast levels in ^{119}Ag were observed before in a measurement of prompt-γ rays following

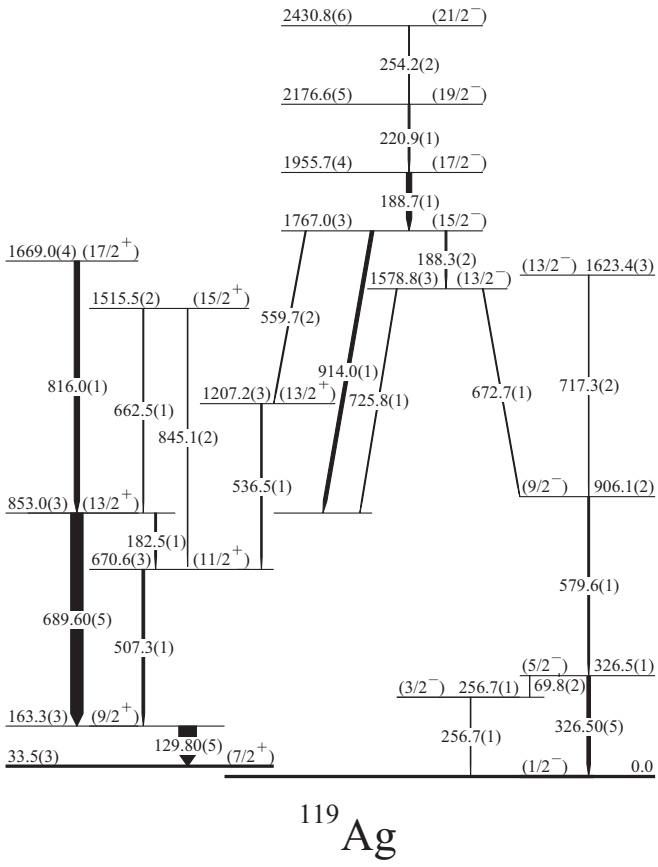

FIG. 10. Partial excitation scheme of ^{119}Ag observed following spontaneous fission of ^{252}Cf, as obtained in the present paper. Energies of levels and transition with their uncertainties are given in keV. Arrow width is approximately proportional to the transition intensity.

spontaneous fission of ^{252}Cf, reported in Ref. [22]. Instrumental in such studies is the use of multidimensional histograms of high dispersion. In our paper we use the so-called, constant-peak-width energy calibration [27], a strongly parabolic function, which allows us to preserve high dispersion in γ spectra also at low γ energies. This and other technical refinements allowed improvements of the data on ^{119}Ag reported in Ref. [22].

New information on ^{119}Ag was obtained by analyzing triple-γ coincidence events from spontaneous fission of ^{252}Cf, measured using the Gammasphere array of Ge detectors [28]. A partial excitation scheme of ^{119}Ag obtained from this analysis is shown in Fig. 10 (the complete level scheme will be published elsewhere).

To the scheme reported in Ref. [22] we add an important level at 1578.8 keV, newly observed in prompt-γ fission data as well as the 256.7-, 326.5-, and 906.1-keV levels reported in β-decay studies. This finding was facilitated by the observation of the 672.7-579.6-326.5-keV and 725.8-689.6-129.8-keV cascades in the present β-decay measurement (see Fig. 5). Double gates set on these cascades show that they are in prompt coincidence with the 189-221-254-keV cascade reported on top of the $(1733.3 + x)$ − keV level [22], indicating

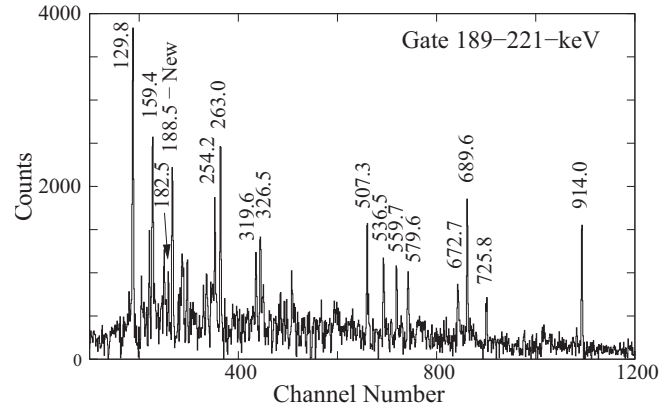

FIG. 11. Coincidence γ spectra doubly gated on lines of ^{119}Ag, as observed in the measurement of spontaneous fission of ^{252}Cf, in the present paper. Line energies are in keV.

that this level decays to the 1578.8-keV level. The x value is here the difference between the $1/2^-$ and $7/2^+$ levels.

In our data we clearly observe the 189-221-254-keV cascade. Figure 11 shows a γ spectrum doubly gated on the 189- and 221-keV lines. In the spectrum one can see the 914.0-keV line, confirming the $(1733.3 + x)$ − keV level reported in Ref. [22] but also lines at 672.7 and 725.8 keV. The expected link to the 1578.8-keV level should have an energy of $(1733 + x - 1579)$ keV $= (154 + x)$ keV. In the spectrum there is a prominent line at 188.5 keV, suggesting that the 189-keV line is a self-coincident doublet. Further analysis provided energies of the two lines in the doublet as shown in Fig. 10.

Figure 12 shows a γ spectrum doubly gated on the 189- and 673-keV lines, in which there are 579.6- and 326.5-keV transitions of the cascade based on the $1/2^-$ level (band A in Fig. 5). The 326.5-579.6-672.7-keV cascade defines the 1578.8-keV level which, on the other hand, decays also to the $7/2^+$ band head (of band B in Fig. 5) via the 725.8-689.6-129.8-keV cascade. The two cascades determine the energy

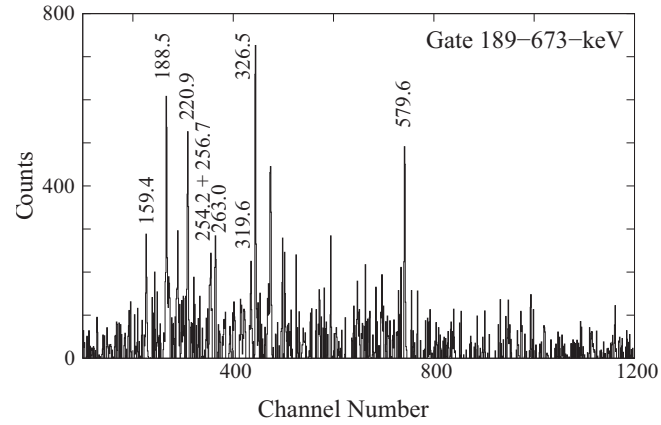

FIG. 12. Coincidence γ spectra doubly gated on lines of ^{119}Ag, as observed in the measurement of spontaneous fission of ^{252}Cf, in the present paper. Line energies are in keV.

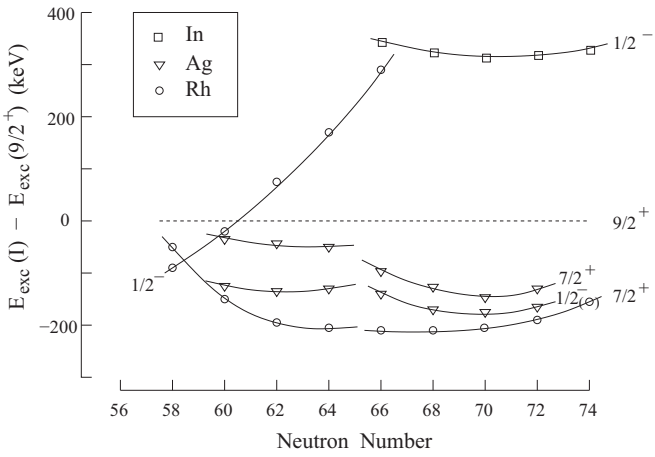

FIG. 13. Systematics of low-energy excitations in odd-A isotopes of Rh, Ag, and In. The data are taken from Ref. [30] and the present paper.

of the $7/2^+$ isomeric band head at 33.5(3) keV above the $1/2^-$ isomer proposed above to be the ground state of ^{119}Ag.

Determination of the $7/2^+$ isomer energy resulting from the spontaneous fission data suggested that we perform a similar analysis of the cascades known from the β-decay data. It resulted in an average energy of the $7/2^+$ state estimated as 33.4(1) keV. Taking a weighted average of the two results we adopted the final value of 33.4(1) keV.

Using the technique described in Ref. [29] we analyzed angular correlations for the 689.6-914.0-keV cascade. The obtained angular correlation coefficients, $A2/A0 = -0.17(5)$ and $A4/A0 = -0.08(8)$, indicate that this is not a cascade of two stretched, quadrupole transitions. Assuming that the 689.6-keV transition is a stretched quadrupole we obtained for the 914.0-keV transition the dipole/quadrupole mixing ratio, δ= 2.1(9) for 13/2-13/2-9/2 spins in the cascade and $\delta = -0.15(10)$ or $-9(5)$ for the 15/2-13/2-9/2 spins.

Spin and parity assignments to levels in ^{119}Ag shown in Fig. 10 are discussed in the next section.

C. Spin-parity assignments to levels in ^{119}Ag and ^{119}Pd

Using the experimental evidence presented in previous sections as well as energy systematics and some general rules we will discuss now spin-parity assignments proposed to levels in ^{119}Ag in Figs. 5 and 10 and then use this information to suggest spins and parities of the β-decaying isomers in ^{119}Pd.

We start with the low-energy β-decaying isomers in ^{119}Ag. Figure 13 shows energies of proton levels in Rh, Ag, and In isotopes, in the region of interest, drawn relative to the $9/2^+$ level corresponding to the $g_{9/2}$ proton excitation and seen in all the nuclei shown in Fig. 13.

The systematics displays rather regular trends for the $1/2^-$ and $7/2^+$ levels in Ag isotopes. We note that when the two isomers in ^{119}Ag are also assigned such spins, the trends extended smoothly up to $N = 72$. The $7/2^+$ and $9/2^+$ assignments to the 33.4- and 163.2-keV levels in ^{119}Ag are supported by our conversion coefficient for the 129.8-keV transition (see Table II). The $7/2^+$ spin-parity assignment to one of the two isomers in ^{119}Ag was previously suggested in other works, as summarized in the compilation in Ref. [23]. Figure 13 shows a similar trend for $7/2^+$ levels in Rh isotopes (in In isotopes low-lying $7/2^+$ levels are not observed).

The compilation in Ref. [23] suggests spin parity $1/2^-$ for the other isomer in ^{119}Ag. This fits well the trend for Ag isotopes and we tentatively assign spin parities of $1/2^-$, $7/2^+$, and $9/2^+$ to the ground state, the 33.4-keV isomer, and the 163.2-keV levels, respectively. We note that the systematics for $1/2^-$ in Rh and In isotopes differs from that for Ag isotopes. These differences will be discussed in the next section.

Spin-parity assignments to higher-energy levels populated in fission of ^{252}Cf can be helped by the commonly observed effect, that fission populates predominantly yrast levels [31]. This implies that spins of excitations populated in fission are growing with the increasing excitation energy. Thus to the strongly populated 853.0- and 1669.0-keV levels we assign, respectively, spin parity $(13/2^+)$ and $(17/2^+)$, in accord with the previous study [22]. The yrast population argument and weaker population of the 670.6-keV level as compared to the 853.0-keV level suggest spin 11/2 for the 670.6-keV level.

Our angular correlation for the 914.0-689.6-keV cascade is consistent with spin 13/2 or 15/2 for the 1767.0-keV level. The yrast population argument and the lack of any decay from this level to the 670.6-keV level favor a tentative (15/2) spin assignment. The missing decay further suggests negative parity for this level. Such assignments were also proposed in Ref. [22]. For 1955.7 and 2176.6 keV we accept spins and parities after Ref. [22] in accord with the yrast population argument and the likely $\Delta I = 1$ character of the low-energy 188.7- and 220.9-keV prompt transitions.

The maximum possible spin of the 1578.8-keV level is 13/2, because of its prompt decay via the 672.7-579.6-326.5-keV cascade to the $1/2^-$ ground state. This is also consistent with the 725.8-keV decay to the 853.0-keV level and the likely $\Delta I = 1$ multipolarity of the new 188.3-keV prompt transition from the 1767.0-keV level. With spin 13/2 negative parity is strongly favored for the 1578.8-keV level.

The 906.1-keV level is also populated by the 717.3-keV transition having intensity comparable to that of the 672.7-keV transition. This is consistent with the 326.6-579.6-717.7-keV cascade forming a stretched-quadrupole band on top of the $1/2^-$ ground state with tentative $5/2^-$, $9/2^-$, and $13/2^-$ spin-parity assignments to the 326.5-, 906.1-, and 1623.4-keV levels, respectively. The 1623.4-keV level is seen only in spontaneous fission data on Fig. 10.

Considering the above spin-parity assignments one can make further assignments to levels populated in β decay, shown in Fig. 5.

The $M1$ multipolarity of the 69.8-keV transition (see Table II) and a weak population of the 256.7-keV level in fission suggest spin $3/2^-$ for this level.

The 136.2-keV link between the 906.4- and 770.2-keV levels and the strong 443.7-keV decay to the $5/2^-$ level at 326.6 keV suggest tentative $(7/2^-)$ assignment to the 770.2-keV level.

The $(13/2^+)$ spin parity of the 1207.2-keV level is consistent with all the data. The alternative $11/2^-$ assignment is less likely because of no decay of this level to the 770.2- and 906.4-keV levels.

For the remaining levels shown in Fig. 5 certain limits for spins are imposed by the branching ratios of their decays and the fact that they are not seen in prompt-γ fission data. This means that they are rather non-yrast and have low spins.

The obtained spin-parity assignments and the $\log_{10} ft$ values shown in Table III put some constraints on spins of β-decaying isomer(s) in ^{119}Pd.

The observation of levels with spins from 3/2 to 13/2 populated in β decay indicates at least two β-decaying isomers in ^{119}Pd, one with low spin and the other with medium spin. The $\log_{10} ft$ values in Table III are typical of nonallowed transitions with spin change $\Delta I = 0, 1$. In particular the $\log_{10} ft$ value of 6.3 determined for the 1579.0-keV level suggests spin 11/2 for the medium spin isomer in ^{119}Pd. Spin 9/2 for this isomer, though less likely, cannot be excluded, considering that the $\log_{10} ft$ values in Table III are in fact lower limits, because of possible additional feeding of levels by many weak, unobserved transitions. The low spin β-decaying isomer in ^{119}Pd may have spin ranging from 1/2 to 5/2. Spin assignments shown in Fig. 5 suggest that the most likely values are 1/2 and 3/2.

III. DISCUSSION

A. β-decaying and low-energy states in ^{119}Pd

The low-lying levels in odd, neutron-rich isotopes of palladium up to ^{117}Pd were discussed in our paper [8]. In ^{117}Pd we postulated new spin parities for the ground and the 203.2-keV long-lived isomeric states to be $1/2^+$ and $7/2^-$, respectively, both corresponding to an oblate deformation.

There are a few model predictions for the ground-state deformation of ^{119}Pd and its even-even neighbors. The potential energy curves (PECs) as a function of the quadrupole deformation parameter β calculated in Ref. [32] for ^{118}Pd and ^{120}Pd in both cases show one flat minimum or two minima, an oblate and a prolate one depending on the method of computing pairing energies used in Ref. [32]. The PECs calculated in Ref. [33] present two very shallow oblate and prolate minima for ^{118}Pd and one flat minimum for ^{120}Pd. The minima become narrower for ^{128}Pd when approaching the closed shell at $N = 82$. The evolution of the β deformation parameter in palladium isotopes calculated in Ref. [33] suggests a slightly prolate shape and spin parity of $3/2^-$ for the ground state of ^{119}Pd. Potential energy surfaces (PESs) calculated as a function of spheroidal and axial-asymmetry shape coordinates (ϵ_2, γ) for $^{118,120}Pd$ [34] show the minima at roughly $(0.2, 48^\circ)$ and $(0.2, 38^\circ)$, respectively. Variation of the β_2 parameter with the neutron number for even-even palladium isotopes presented in Ref. [35] ends at $\beta_2 \approx 0.21$ for ^{118}Pd, and the systematic trend suggests $\beta_2 \leqslant 0.2$ for ^{119}Pd. Two model predictions [36,37] show negative values of the β_2 parameter, thus the preference for an oblate shape of the ground state. In Ref. [36] there are two β_2 values for each nucleus due to two sets of the force parameters used. Thus for ^{118}Pd the β_2 are -0.198 and -0.184 and for ^{120}Pd they decrease to -0.163 and -0.151. According to Ref. [37] $\beta_2 = -0.206$ for ^{119}Pd.

The mentioned theoretical calculations point to the absolute value of the quadrupole deformation parameter $|\beta_2| \approx 0.2$. The model predictions of oblate and prolate minima suggest coexisting shapes with the opposite sign of the deformation for the ground and isomeric states in ^{119}Pd. In fact, the model of Ref. [33] predicts oblate isomeric states and prolate ground states in palladium isotopes for $A = 114$–117. However, the latter are not in full agreement with our experimental results on ^{117}Pd [8].

The systematics of the low-lying and isomeric states in odd-A palladium isotopes shown in Fig. 7 of Ref. [8] evolves smoothly for $A = 105$–115. The level structure of ^{117}Pd is qualitatively different and does not fully fit a simple extension of the systematics of the lighter odd-A palladium isotopes, making the systematic predictions for ^{119}Pd difficult. One may suggest, based on Figs. 6 and 8 of Ref. [8], that the medium-spin isomeric state in ^{119}Pd will have spin $11/2^-$ and be positioned above the ground state. However, for the ground state in ^{119}Pd the prediction is less clear, with Fig. 6 of Ref. [8] pointing to spin parity $1/2^+$ or $3/2^+$.

Further hints can be obtained from properties of odd-A cadmium isotopes neighboring the discussed palladium nuclei. Their systematics shown in Fig. 14 extends to higher N values, and thus is more reliable at $N = 73$. It is also expected that the neutron-rich cadmium isotopes, which are near the $Z = 50$ shell closure, will have oblate deformation in their ground states, similar to the expectations for ^{117}Pd and ^{119}Pd nuclei.

In the lighter cadmium isotopes up to ^{119}Cd the ground state has spin parity $1/2^+$; for an experimental determination of the spin values see Ref. [38]. In ^{121}Cd, the isotone of ^{119}Pd, the ground-state spin parity changes to $3/2^+$, and $1/2^+$ becomes the lowest excited state. The trend of increasing energy of the $1/2^+$ level continues in ^{123}Cd. We note that the energy of the $11/2^-$ isomeric level relative to the $3/2^+$ state in odd-A cadmium isotopes increases above the neutron number $N = 67$, similarly as observed in Fig. 6 of Ref. [8] for their palladium isotones. This suggests similar structures of these Pd and Cd isotones and suggests spin parity $1/2^+$ or $3/2^+$ for the ground state of ^{119}Pd. We note that in the single-neutron Nilsson (see, e.g., Fig. 9 in Ref. [40]) diagrams there are 1/2 and 3/2 positive parity levels, stemming from the $2d_{3/2}$ shell, which can be occupied by the 73rd neutron for both oblate and prolate deformation not exceeding $|\beta_2| \approx 0.2$. Additionally there is the $1/2^+$ level from the $3s_{1/2}$ orbital for an oblate shape.

One can now combine the above information with the new observation of the 18.7-219.8-keV cascade discussed in Sec. II A 5 to propose a hypothetical scheme of low-energy excitations in ^{119}Pd.

Figure 15(a) shows again systematics of some of the excitation energies in odd-A palladium and cadmium isotopes displayed in Fig. 14 above and in Fig. 6 of Ref. [8] but now drawn relative to the lowest $3/2^+$ level observed in these nuclei. Once more one sees a similar trend in palladium and

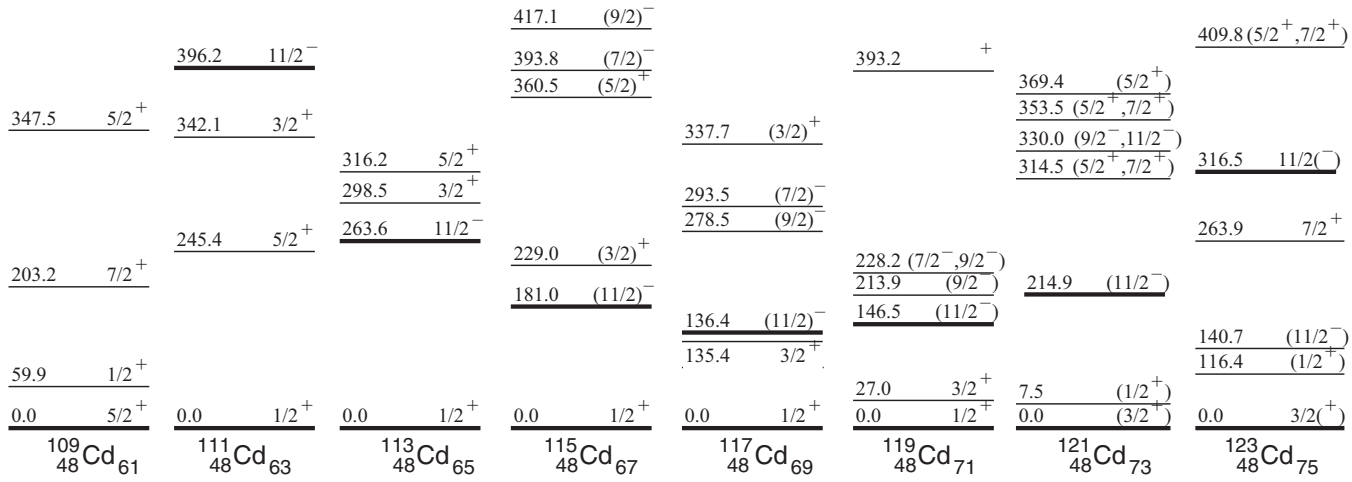

FIG. 14. Systematics of the selected low-energy levels in odd-A nuclei of cadmium, the isotones of palladium. Data are taken from Ref. [30], except for the ground and isomeric states in ^{123}Cd [39].

cadmium isotopes, which support an extension of the palladium systematics to $N = 73$.

This extension suggests in ^{119}Pd a $1/2^+$ level very close to the $3/2^+$ state, a $5/2^+$ excited level at about 250 keV above the ground state, and a $11/2^-$ about 350 keV above the ground state. In Fig. 15(b) we have drawn (to scale) a hypothetical excitation scheme comprising the four levels and the newly found 18.7-219.8-keV cascade. The lack of the crossover decay from the $5/2^+$ level to the ground state suggests spin $3/2^+$ for the 18.7-keV level.

The unobserved isomeric electromagnetic decay, X from the $11/2^-$ isomer with the proposed half-life of 0.85 s, has an energy of about 100 keV and $E3$ multipolarity. It feeds the 238.5-keV $5/2^+$ level but is not seen in coincidence with the 18.7-219.8-keV cascade most likely because of its high total conversion coefficient which for an $E3$ transition of 100 keV yields $\alpha_{\text{tot}} \approx 20$.

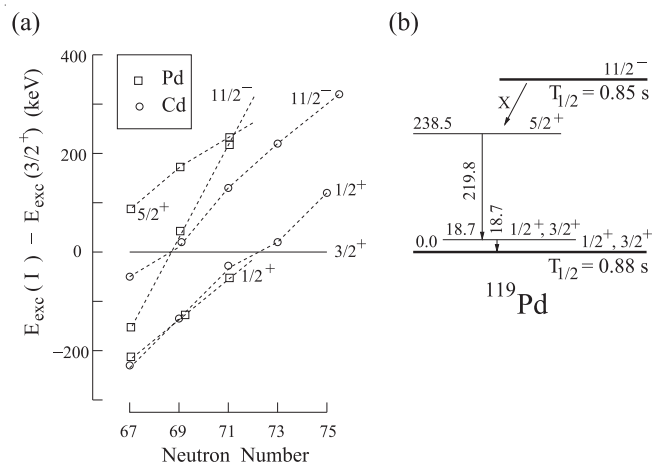

FIG. 15. (a) Systematics of low-energy excitations in odd-A isotopes of Pd and Cd. (b) Scheme of low-energy excitations in ^{119}Pd proposed in this paper. The data are taken from Ref. [30] and the present paper.

Taking a single-particle rate estimate for an $E3$ transition of 100 keV of about 10^{-2} s^{-1} and the above α_{tot} value one gets a rough estimate for the associated half-life of a few seconds. This has to be corrected for the unknown β-decay branch and a possible hindrance, which is observed in lighter odd-A palladium isotopes [8] but one can see that using such a rough estimate it is possible to reproduce the observed half-life of 0.85 s.

Interestingly, to reproduce this half-life one should use in ^{119}Pd a much smaller hindrance factor than observed in lighter Pd isotopes, where it is of the order of 10^3 [8] and is thought to be due to different shapes of the initial and final levels in the decay. This would then imply that in ^{119}Pd these shapes are not different. The $11/2^-$ isomer corresponds to an oblate $11/2[505]$ orbital. However, the $5/2^+$ levels in lighter Pd isotopes are prolate. We then conclude that in ^{119}Pd the $5/2^+$ level is oblate.

At the end let us point to some puzzling observations concerning the discussed isomers. The $\log_{10} ft$ value of 5.7 for the $5/2^-$ 326.5-keV and $7/2^-$ 770.2-keV levels in ^{119}Ag indicates the allowed character of the corresponding β transition from an isomer in ^{119}Pd, thus suggesting spin $5/2^-$ or $7/2^-$ for such a state. One could propose a third β-decaying isomer in ^{119}Pd with spin $5/2^-$. Such a low-energy level could correspond to the $5/2^-$ orbital originating from the $h_{11/2}$ shell in an oblate potential. In principle such an isomer could also account for feeding other low-spin states in ^{119}Ag, without the need for a $(1/2^+, 3/2^+)$ β-decaying isomer. However, this would mean that the systematics for Pd isotopes shown in Fig. 15 breaks at $N = 73$ and is quite different than in Cd isotopes.

It is of high interest to continue detailed studies of nuclei in this region in order to resolve the above puzzle and other mysteries like the mentioned very high variations of hindrance factors of $E3$ decays from $11/2^-$ isomers in odd-A palladium isotopes.

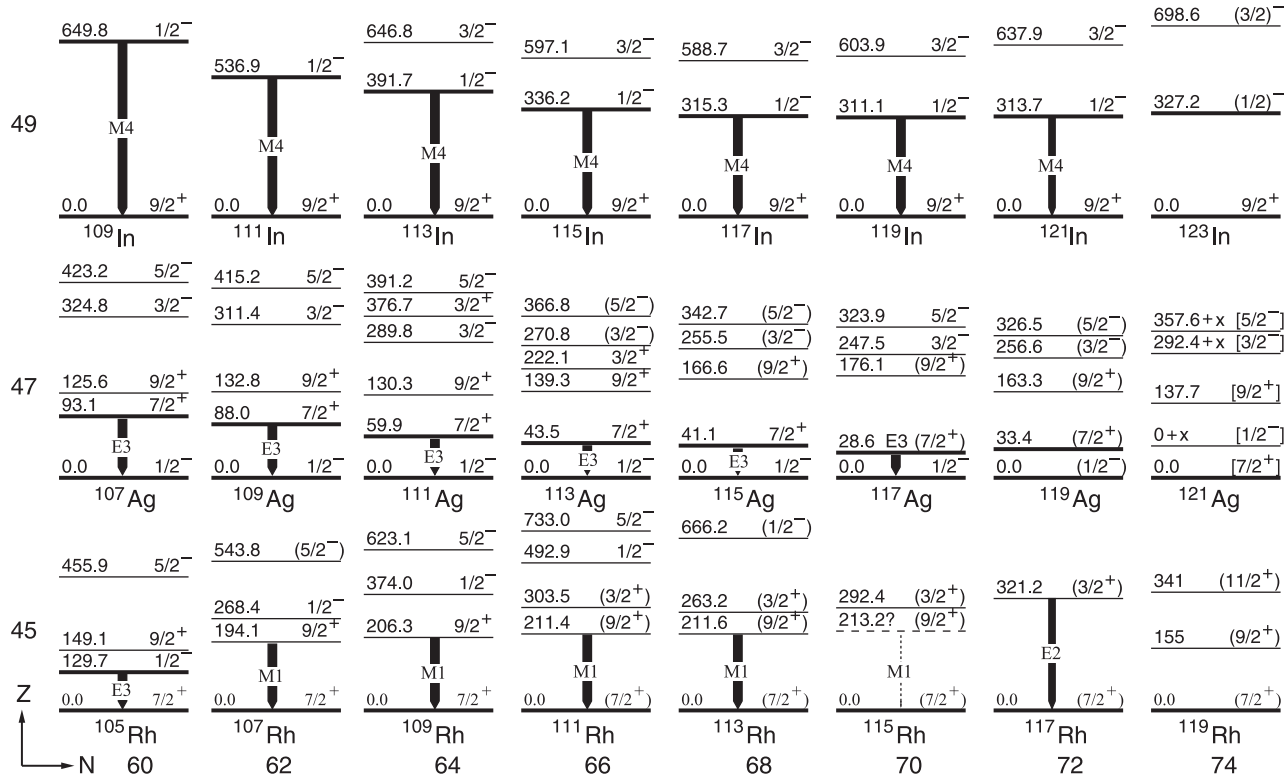

FIG. 16. Systematics of the selected low-energy levels in odd-A nuclei of rhodium, silver, and indium. The data are taken from Ref. [30] and the present paper. Spin-parity assignments in ^{121}Ag were proposed in Ref. [41] based solely on the systematics reported in Refs. [11,42].

B. β-decaying and other possible isomers in ^{119}Ag

The $7/2^+$ spin and parity for the β-decaying state of ^{119}Ag comes from the study of its decay to ^{119}Cd [20]. The assignment was proposed as the one most conforming with the systematics. The same $7/2^+$ assignment was proposed for the ground state of ^{119}Ag in the first β-decay study at the IGISOL [11].

The calculation of PES [22] suggests the $7/2^+[413]$ Nilsson orbital assignment to the ground state of ^{119}Ag with a prolate deformation of $\beta_2 \approx 0.1$. A low-energy $1/2^-[301]$ level having a nonaxial deformation close to an oblate shape was predicted in ^{119}Ag at 8 keV. The small energy difference, calculated between the $7/2^+$ ground state and the $1/2^-$ excited level, fits well the difference of 33.4 keV measured in the present paper. However, the spin of the ground state has been determined in this paper to be $1/2^-$ and the 33.4-keV isomer is assigned spin $7/2^+$.

No γ decay from the $7/2^+$ level at the bottom of band B to the $1/2^-$ ground level has been found in our data. Such a low-energy $E3$ transition would be strongly converted; the $\alpha_{\rm tot}(E3, 33.4\ {\rm keV})$ is close to 4900 [24]. Therefore in the previous IGISOL study [11,13] it was thoroughly searched for in a conversion electron measurement but without success.

It is interesting to note that following Refs. [11,20] the $7/2^+$ spin assignment was proposed for the ground state of ^{121}Ag [41], as shown in Fig. 16 displaying low-energy levels in odd-A rhodium, silver, and indium isotopes, which extends the systematics shown in Fig. 13. With the $1/2^-$ spin of the ground state in ^{119}Ag the proposition of Ref. [41] may be questioned. We note that the systematics of $1/2^-$ levels in neutron-rich silver isotopes, shown in Fig. 13, is quite regular. The energy variation of this level is very small, which may be expected for a level corresponding to a given, low-spin proton orbital in a chain of isotopes. It is then possible that the ground state of ^{121}Ag may have spin $1/2^-$. This expectation is supported by the systematics of $1/2^-$ levels in indium isotopes, extending up to $N = 74$, as seen in Fig. 13 (the position of $1/2^-$ levels in indium above the $9/2^+$ level is due to the rise of the Fermi level towards the $9/2[404]$ orbital when moving from $Z = 47$ to 49).

One more effect seen in Fig. 13 worth mentioning is the different trend of $1/2^-$ levels in Rh isotopes. This is probably due to higher prolate deformation in these nuclei, as compared to Ag isotopes. A somewhat weaker but visible effect is the change of the trends above the neutron midshell at $N = 64$, probably connected with the decrease of prolate deformation. It would be interesting to find how $1/2^-$ levels in rhodium isotopes behave there.

In Ref. [22] another low-energy level with a nonaxial deformation, corresponding to the $1/2^+[440]$ configuration, was predicted in ^{119}Ag at 25 keV. No candidate for such low-energy level was found in the present paper.

Finally, we note that in odd-A Tc, Rh, and Ag isotopes one observes a strongly deformed $1/2^+[431]$ intruder state, which forms isomers in some of these nuclei. This steeply down-sloping orbital appears at the prolate side of the Nilsson diagram. In neutron-rich silver isotopes a rotational band built

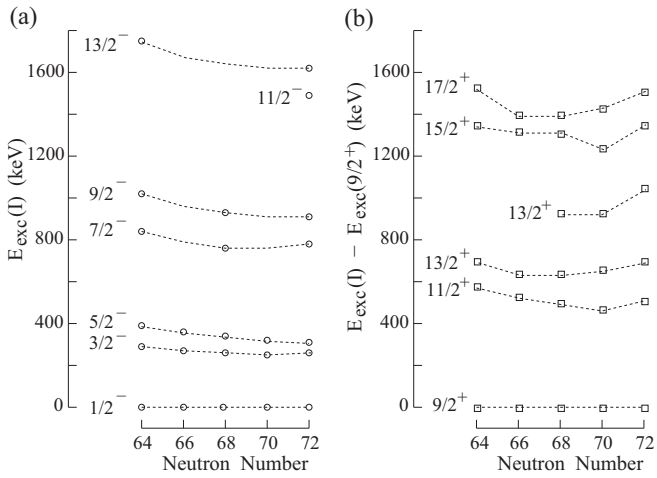

FIG. 17. (a) Systematics of rotational bands in odd-A Ag isotopes built on top of (a) the $1/2^-$ level and (b) the $9/2^+$ level. The data are taken from Refs. [30,43] and the present paper.

on the $1/2^+[431]$ configuration is observed in ^{109,111,113,115}Ag nuclei (see systematics of these bands shown in Fig. 8 of Ref. [43]). To date such bands were not seen in ^{117}Ag either in β-decay [11,30] or in spontaneous fission studies [44]. They are also not seen in ^{119}Ag in the present paper. This suggests a small or nonexistent prolate deformation of ^{119}Ag. It is in accord with the low, positive value of quadrupole deformation, $\beta_2 \approx 0.1$, predicted for the ground state in Ref. [22]. It is also consistent with the oblate deformation of $\beta_2 = -0.227$, calculated in Ref. [37]. An intriguing question is whether the 617.6-keV isomeric transition, suggested to be in ^{119}Pd, could actually correspond to a decay of the $1/2^+[431]$ configuration in ^{119}Ag.

C. Levels on top of the $1/2^-$ ground state in ^{119}Ag

In our study of ^{115}Ag [43] a general discussion of negative parity levels in odd silver isotopes was presented, including systematics of the relevant states up to ^{117}Ag. Using the results for ^{119}Ag obtained in the present paper we extended the systematics of collective, rotational bands shown in Fig. 6 of Ref. [43] to neutron number $N = 72$. The updated picture is shown in Fig. 17.

In the systematics shown in Figs. 16 and 17(a), the $3/2^-$ and $5/2^-$ members of the ground-state band show a smooth energy variation. The 256.6- and 326.5-keV levels of ^{119}Ag, assigned spins $3/2^-$ and $5/2^-$, fit well the trend. We propose that they are members of the collective band based on the $1/2^-$ excitation. This is a weakly deformed, decoupled band with the unfavored branch shifted up in energy. The $7/2^-$ and $9/2^-$ members of this band in ^{119}Ag, proposed at 770.2 and 906.4 keV, respectively, fit well the trend of analogous excitations in ^{111}Ag and ^{115}Ag. It is of interest to identify such excitations in ^{113}Ag and ^{117}Ag isotopes. We further propose that the 1440.5- and 1623.4-keV levels found in ^{119}Ag are the $11/2^-$ and $13/2^-$ members of this band. The $13/2^-$ level is observed at similar excitation energy in ^{111}Ag. It is of interest to identify analogous $11/2^-$ and $13/2^-$ levels in other Ag isotopes. The 1157.8-keV level linked to the 1440.5-keV level by a low-energy transition has probably spin $9/2$ and may be linked to the discussed rotation structure. Such a spin means that the 1157.0-keV γ transition to the $1/2^-$ level, which was proposed by an approximate energy matching, only, should be ignored.

Other levels of possible negative parity observed in band A may be due to single-particle proton excitations to the nearby $3/2^-$ level originating from the $2p_{3/2}$ shell or $3/2^-$ and $5/2^-$ levels originating from the $1f_{5/2}$ shell.

The 607.1-keV level in ^{115}Ag was interpreted as the $\pi 3/2^-[301]$ Nilsson state originating from the $1f_{5/2}$ shell [43]. The systematics of $3/2^-$ levels corresponding to the $\pi 3/2^-[301]$ excitation seen in Fig. 6 in Ref. [43] shows a shallow minimum at $N = 66$. Therefore, in ^{119}Ag one may expect the respective level to appear above 600 keV but below 800 keV. The 686.2-keV level seen in Fig. 5 decays by a strong 686.2-keV transition to the $1/2^-$ ground state. It also deexcites by the 359.8- and 429.7-keV transitions to $5/2^-$ and $3/2^-$ levels at 326.5 and 256.6 keV, respectively. It is the same decay pattern as observed for the 642- and 607-keV levels in ^{111}Ag and ^{115}Ag, both interpreted as the $3/2^-[301]$ proton excitation. Therefore, we propose the same $3/2^-[301]$ proton configuration for the 686.2-keV level in ^{119}Ag.

The 787.7-keV level in ^{115}Ag was interpreted as the $\pi 5/2^-[303]$ proton excitation stemming from the $1f_{5/2}$ shell [43]. Its similarity to the 809.2-keV level in ^{111}Ag of the same configuration was pointed out, too. The systematics of $5/2^-$ levels corresponding to the $\pi 5/2^-[303]$ configuration, shown in Fig. 6 in Ref. [43], suggests that a candidate for such a state in ^{119}Ag should be located between 800 and 1000 keV. In Fig. 5 one sees a level at 1032.1 keV, which deexcites to the $5/2^-$ level at 326.5 keV, though this decay branch is weaker than in ^{111,115}Ag.

There are several levels populated in β decay of ^{119}Pd with $\log_{10} ft$ values of about 6.2, a value between allowed and first forbidden transitions. Because these $\log_{10} ft$ values represent lower limits, the forbidden character of the β feeding is more likely. Alternatively, there may be some retardation due to the decay to a complex, collective nature of the final state. We note that apart from collective rotations collective vibrations are also possible. In a weakly deformed nucleus as ^{119}Ag, quadrupole vibrations may exhibit higher excitation energy than the first quadrupole rotational excitation. Such collective excitations may be built on top of the single-particle configurations, discussed above.

Finally, the 1579.0-, 1663.2-, 1803.7-, 1811.1- and 1888.5-keV levels, which deexcite to the 906.4-keV level, probably have spin equal to or higher than $9/2$. They may correspond to three-quasiparticle (q.p.) excitations. Such excitations were reported in odd-A silver isotopes. In Ref. [22] a three-q.p. oblate configuration was proposed for the band on top of the 1767.0-keV level (1733 keV + X in Ref. [22]). The 188.3-keV level favored low-energy decay of this level to the 1579.0-keV level strongly suggests a three-q.p. nature of the 1579.0-keV level. We note that there are more three-q.p. configurations around this energy, as seen in Ref. [22]. Therefore

some of the 1663.2-, 1803.7-, 1811.1-, and 1888.5-keV levels may also correspond to various three-q.p. excitations.

D. Levels on top of the $7/2^+$ isomer in ^{119}Ag

The $7/2^+$ levels which show similar behavior in Rh and Ag isotopes were interpreted as $\pi(g_{9/2})^n_{7/2}$ configuration, a type of the $(j^3)_{j-j}$ "anomalous" coupling, as observed in ^{87}Se [45], with three proton holes in Ag isotopes. Alternatively, it could be seen as $\pi 7/2^+[413]$ excitation in ^{119}Ag. However, in the ^{115,117,119,121,123}In isotopes [23,46], which have one proton hole in the $g_{9/2}$ shell, the $7/2^+$ levels appear well above their $9/2^+$ ground states, which favors the former interpretation. It is likely that both configurations are admixed in these $7/2^+$ levels.

As seen in Fig. 13 just above the $7/2^+$ level there is a $9/2^+$ level in all odd-A isotopes, which most likely corresponds to a rather pure single-particle excitation $9/2^+[404]$ proton configuration. This is a bandhead for rotational bands. There is a rich systematics of rotational levels built on top of the $9/2^+[404]$ proton configuration in odd-A silver isotopes, as shown in Fig. 17(b). In ^{119}Ag this rotational band comprises the 670.6-, 853.0-, 1515.5-, and 1669.0-keV levels, seen in spontaneous fission data. As seen in Fig. 17 all these levels have counterparts in lighter Ag isotopes and the systematic trends are quite regular with small deviations of the $15/2^+$ level.

The 713.9- and the 1170.3-keV levels of band B may be due to a rotation built on top of the $\pi(g_{9/2})^3_{7/2}$ configuration. It is of interest to search for such bands in lighter Ag isotopes.

The $13/2^+$ level at 1207.2-keV level has counterparts in ^{115}Ag and ^{117}Ag, which show a similar, exclusive decay to the $13/2^+$ yrast state and have similar excitation energies, as seen in Fig. 17(b). This suggests that all three levels have the same configuration. However, the levels in ^{115}Ag and ^{117}Ag were assigned negative parity [22]. We note that a $13/2^-$ excitation of 1207.2 keV in ^{119}Ag would be more yrast than other $13/2^-$ levels in this nucleus, including the proposed yrast rotational level at 1623.4 keV. Because it is unlikely that a level at about 1.2 MeV corresponds to a three-q.p. excitation we propose that these 13/2 levels have positive parity in all three, ^{115}Ag, ^{117}Ag, and ^{119}Ag, nuclei. Further work is needed to explain their nature.

In the band B there are five levels at energies seen above 2 MeV in Fig. 5, the highest one at 2818.4 keV. Each of them is coincident with γ 129.8-keV transition. The 2161.8-keV level also shows a weak γ transition to the 33.4-keV isomeric state. These levels are fed with $\log_{10} ft$ values between 5.7 and 6.0 if no ground state feeding is assumed (6.0 to 6.3 if 50% ground-state feeding). Not much can be said about them because of the wide range of their possible spins. At this excitation energy these levels are probably three-q.p. in nature.

IV. SUMMARY

Neutron-rich ^{119}Pd and ^{119}Ag nuclei were studied in β decay of mono-isotopic samples of ^{119}Pd obtained using the IGISOL and Penning trap techniques at the Accelerator Laboratory of the University of Jyväskylä. Measurement of $\gamma\gamma$ and $\beta\gamma$ coincidences following β decay of ^{119}Pd has revealed two distinct level structures in ^{119}Ag, based on the $1/2^-$ and $7/2^+$ isomers reported previously. To find relative positions of these isomers we analyzed triple-γ coincidences of prompt-γ rays following spontaneous fission of ^{252}Cf, measured using the Gammasphere detector array at the Argonne National Laboratory. A new, medium-spin level found at 1578.8 keV, which decays to both structures observed in β decay, allowed us to determine positions of the isomers. Contrary to previous suggestions, our data place the $1/2^-$ isomer 33.4 keV below the $7/2^+$ and we propose it as a new ground state of ^{119}Ag. Extended energy systematics suggest that the same sequence of isomeric states may be present in ^{121}Ag in contrast to previous reports.

Analysis of level feeding in ^{119}Ag following β decay of ^{119}Pd indicated that there are at least two β-decaying isomers in ^{119}Pd, one with probable $11/2^-$ spin and a half-life of 0.85 s and the other with low spin, probably $1/2^+$ or $3/2^+$ and a half-life of 0.88 s. A newly observed γ cascade of 18.7-219.8-keV transitions, populated in an IT decay of an unknown isomer, was proposed in ^{119}Pd. The cascade may be populated by a low-energy, $E3$ isomeric transition with a low hindrance factor, decaying from the $11/2^-$ isomer. This picture fits well the energy systematics of odd-A Pd and Cd isotopes in the region. However, $\log_{10} ft$ values of some of the levels in ^{119}Ag obtained in this paper suggest that there may be a third β-decaying isomer with probable spin $5/2^-$, which would invalidate this scenario. Clearly, more detailed study is needed to resolve this puzzle as well as to explain strongly varying hindrances of the $E3$, IT transitions observed in odd-A Pd isotopes and probably connected to the deformation change with the increasing neutron number and the coexistence of prolate and oblate shapes in these nuclei.

Energies of levels observed in ^{119}Ag, which fit well smooth trends established by lighter Ag isotopes, were interpreted as proton excitations with collective, rotational bands on top of them. The observed properties of excitations suggest weak oblate deformation of levels in ^{119}Ag, which is supported by the calculations reported in other works.

Solving the puzzle of the isomers in the $A = 119$ palladium and silver isotopes can be facilitated with the Phase-Imaging Ion-Cyclotron-Resonance (PI-ICR) method [47], which is capable to resolve close-lying isomeric states. The PI-ICR method was commissioned at the JYFLTRAP Penning trap [48] and its feasibility in separation of isomers in some indium isotopes was already demonstrated [49].

ACKNOWLEDGMENTS

A.K. acknowledges support from the Academy of Finland under Projects No. 275389, No. 284516, and No. 312544, as well as the funding from the European Union's Horizon 2020 research and innovation program under Grant No. 771036 (ERC Consolidator Grant MAIDEN). T.E. acknowledges support from the Academy of Finland under Projects No. 295207 and No. 306980. Access to the research facilities was supported by the European Union's Horizon 2020 research and innovation program under Grant No. 654002 (ENSAR2).

[1] R. F. Casten, *Nuclear Structure from a Simple Perspective* (Oxford University, New York, 2000).

[2] J. L. Wood, K. Heyde, W. Nazarewicz, M. Huyse, and P. van Duppen, Phys. Rep. **215**, 101 (1992).

[3] W. Urban, T. Rząca-Urban, J. L. Durell, W. R. Phillips, A. G. Smith, B. J. Varley, I. Ahmad, and N. Schulz, Eur. Phys. J. A **20**, 381 (2004).

[4] W. Urban, T. Rząca-Urban, J. L. Durell, A. G. Smith, and I. Ahmad, Eur. Phys. J. A **24**, 161 (2005).

[5] J. Kurpeta, W. Urban, A. Płochocki, J. Rissanen, J. A. Pinston, V.-V. Elomaa, T. Eronen, J. Hakala, A. Jokinen, A. Kankainen, P. Karvonen, I. D. Moore, H. Penttilä, A. Saastamoinen, C. Weber, and J. Äystö, Phys. Rev. C **84**, 044304 (2011).

[6] J. Kurpeta, W. Urban, A. Płochocki, T. Rząca-Urban, A. G. Smith, J. F. Smith, G. S. Simpson, I. Ahmad, J. P. Greene, A. Jokinen, and H. Penttilä, Phys. Rev. C **90**, 064315 (2014).

[7] J. Kurpeta, J. Rissanen, A. Płochocki, W. Urban, V.-V. Elomaa, T. Eronen, J. Hakala, A. Jokinen, A. Kankainen, P. Karvonen, T. Małkiewicz, I. D. Moore, H. Penttilä, A. Saastamoinen, G. S. Simpson, C. Weber, and J. Äystö, Phys. Rev. C **82**, 064318 (2010).

[8] J. Kurpeta, A. Płochocki, W. Urban, T. Eronen, A. Jokinen, A. Kankainen, V. S. Kolhinen, I. D. Moore, H. Penttilä, M. Pomorski, S. Rinta-Antila, T. Rząca-Urban, and J. Wiśniewski, Phys. Rev. C **98**, 024318 (2018).

[9] J. Kurpeta, A. Płochocki, W. Urban, A. Abramuk, L. Canete, T. Eronen, A. Fijałkowska, S. Geldhof, K. Gotowicka, A. Jokinen, A. Kankainen, I. D. Moore, D. Nesterenko, H. Penttilä, I. Pohjalainen, M. Pomorski, M. Reponen, S. Rinta-Antila, A. de Roubin, T. Rząca-Urban *et al.* Phys. Rev. C **100**, 034316 (2019).

[10] W. Urban, T. Rząca-Urban, J. Wiśniewski, J. Kurpeta, A. Płochocki, J. P. Greene, A. G. Smith, and G. S. Simpson, Phys. Rev. C **102**, 024318 (2020).

[11] H. Penttilä, J. Äystö, K. Eskola, Z. Janas, P. P. Jauho, A. Jokinen, M. E. Leino, J. M. Parmonen, and P. Taskinen, Z. Phys. A **338**, 291 (1991).

[12] F. Montes, A. Estrade, P. T. Hosmer, S. N. Liddick, P. F. Mantica, A. C. Morton, W. F. Mueller, M. Ouellette, E. Pellegrini, P. Santi, H. Schatz, A. Stolz, B. E. Tomlin, O. Arndt, K.-L. Kratz, B. Pfeiffer, P. Reeder, W. B. Walters, A. Aprahamian, and A. Wöhr, Phys. Rev. C **73**, 035801 (2006).

[13] H. Penttilä, Ph.D. thesis, Department of Physics, University of Jyväskylä, Research Report No. 1/1992, 1992 (unpublished).

[14] I. Moore, T. Eronen, D. Gorelov, J. Hakala, A. Jokinen, A. Kankainen, V. Kolhinen, J. Koponen, H. Penttilä, I. Pohjalainen, M. Reponen, J. Rissanen, A. Saastamoinen, S. Rinta-Antila, V. Sonnenschein, and J. Äystö, Nucl. Instr. Meth. Phys. Res. B **317**, 208 (2013).

[15] P. Karvonen, I. D. Moore, T. Sonoda, T. Kessler, H. Penttilä, K. Peräjärvi, P. Ronkanen, and J. Äystö, Nucl. Instr. Meth. Phys. Res. B **266**, 4794 (2008).

[16] A. Nieminen, J. Huikari, A. Jokinen, J. Äystö, P. Campbell, and E. Cochrane, Nucl. Instrum. Methods Phys. Res. A **469**, 244 (2001).

[17] G. Savard, St. Becker, G. Bollen, H.-J. Kluge, R. B. Moore, Th. Otto, L. Schweikhard, H. Stolzenberg, and U. Wiess, Phys. Lett. A **158**, 247 (1991).

[18] T. Eronen, V. S. Kolhinen, V.-V. Elomaa, D. Gorelov, U. Hager, J. Hakala, A. Jokinen, A. Kankainen, P. Karvonen, S. Kopecky, I. D. Moore, H. Penttilä, S. Rahaman, S. Rinta-Antila, J. Rissanen, A. Saastamoinen, J. Szerypo, C. Weber, and J. Äystö, Eur. Phys. J. A **48**, 46 (2012).

[19] V. S. Kolhinen, T. Eronen, D. Gorelov, J. Hakala, A. Jokinen, K. Jokiranta, A. Kankainen, M. Koikkalainen, J. Koponen, H. Kulmala, M. Lantz, A. Mattera, I. D. Moore, H. Penttilä, T. Pikkarainen, I. Pohjalainen, M. Reponen, S. Rinta-Antila, J. Rissanen, C. R. Triguero, J. Äystö, *et al.*, Nucl. Instr. Meth. Phys. Res. B **317**, 506 (2013).

[20] Y. Kawase, B. Fogelberg, J. McDonald, and A. Bäcklin, Nucl. Phys. A **241**, 237 (1975).

[21] Meng Wang, W. J. Huang, F. G. Kondev, G. Audi, and S. Naimi, Chin. Phys. C **45**, 030003 (2021).

[22] E. H. Wang, J. H. Hamilton, A. V. Ramayya, Y. X. Liu, H. J. Li, A. C. Dai, W. Y. Liang, F. R. Xu, J. K. Hwang, S. H. Liu, N. T. Brewer, Y. X. Luo, J. O. Rasmussen, Y. Sun, S. J. Zhu, G. M. Ter-Akopian, and Yu. Ts. Oganessian, Phys. Rev. C **95**, 064311 (2017).

[23] D. M. Symochko, E. Browne, and J. K. Tuli, Nucl. Data Sheets **110**, 2945 (2009).

[24] T. Kibèdi, T. W. Burrows, M. B. Trzhaskovskaya, P. M. Davidson, and C. W. Nestor, Jr., Nucl. Instr. Meth. Phys. Res. A **589**, 202 (2008).

[25] National Nuclear Data Center, www.nndc.bnl.gov/logft/

[26] J. Kantele, *Handbook of Nuclear Spectrometry* (Academic Press, London, 1995).

[27] W. Urban, M. Jentschel, B. Märkisch, Th. Materna, Ch. Bernards, C. Drescher, Ch. Fransen, J. Jolie, U. Köster, P. Mutti, T. Rząca-Urban, and G. S. Simpson, JINST **8**, P03014 (2013).

[28] I.-Y. Lee, Nucl. Phys. A **520**, c641 (1990).

[29] H. Naïdja, F. Nowacki, B. Bounthong, M. Czerwiński, T. Rząca-Urban, T. Rogiński, W. Urban, J. Wiśniewski, K. Sieja, A. G. Smith, J. F. Smith, G. S. Simpson, I. Ahmad, and J. P. Greene, Phys. Rev. C **95**, 064303 (2017).

[30] Evaluated Nuclear Structure Data File, https://www.nndc.bnl.gov/ensdf/

[31] I. Ahmad and W. R. Phillips, Rep. Prog. Phys. **58**, 1415 (1995).

[32] J. Skalski, S. Mizutori, and W. Nazarewicz, Nucl. Phys. A **617**, 282 (1997).

[33] P. Sarriguren, Phys. Rev. C **91**, 044304 (2015).

[34] P. Möller, A. J. Sierk, R. Bengtsson, H. Sagawa, and T. Ichikawa, At. Data Nucl. Data Tables **98**, 149 (2012).

[35] S. Lalkovski, A. M. Bruce, A. Jungclaus, M. Górska, M. Pfützner, L. Cáceres, F. Naqvi, S. Pietri, Zs. Podolyák, G. S. Simpson, K. Andgren, P. Bednarczyk, T. Beck, J. Benlliure, G. Benzoni, E. Casarejos, B. Cederwall, F. C. L. Crespi, J. J. Cuenca-García, I. J. Cullen, A. M. Denis Bacelar, P. Detistov *et al.* Phys. Rev. C **87**, 034308 (2013).

[36] M. Bhuyan, Phys. Rev. C **92**, 034323 (2015).

[37] P. Möller, A. J. Sierk, T. Ichikawa, and H. Sagawa, At. Data Nucl. Data Tables **109-110**, 1 (2016).

[38] D. T. Yordanov, D. L. Balabanski, J. Bieroń, M. L. Bissell, K. Blaum, I. Budinčević, S. Fritzsche, N. Frömmgen, G. Georgiev, Ch. Geppert, M. Hammen, M. Kowalska, K. Kreim, A. Krieger, R. Neugart, W. Nörtershäuser, J. Papuga, and S. Schmidt, Phys. Rev. Lett. **110**, 192501 (2013).

[39] A. Kankainen, J. Hakala, T. Eronen, D. Gorelov, A. Jokinen, V. S. Kolhinen, I. D. Moore, H. Penttilä, S. Rinta-Antila, J. Rissanen, A. Saastamoinen, V. Sonnenschein, and J. Äystö, Phys. Rev. C **87**, 024307 (2013).

[40] R. A. Meyer, E. Monnand, J. A. Pinston, F. Schussler, I. Ragnarsson, B. Pfeiffer, H. Lawin, G. Lhersonneau, T. Seo, and K. Sistemich, Nucl. Phys. A **439**, 510 (1985).

[41] I. Stefanescu, W. B. Walters, P. F. Mantica, B. A. Brown, A. D. Davies, A. Estrade, P. T. Hosmer, N. Hoteling, S. N. Liddick, W. D. M. Rae, T. J. Mertzimekis, F. Montes, A. C. Morton, W. F. Mueller, M. Ouellette, E. Pellegrini, P. Santi, D. Seweryniak, H. Schatz, J. Shergur *et al.*, Eur. Phys. J. A **42**, 407 (2009).

[42] B. Fogelberg, E. Lund, Ye. Zongyuan, and B. Ekström, AIP Conf. Proc. **164**, 296 (1987).

[43] J. Rissanen, J. Kurpeta, V.-V. Elomaa, T. Eronen, J. Hakala, A. Jokinen, A. Kankainen, I. D. Moore, H. Penttilä, A. Płochocki, A. Saastamoinen, W. Urban, C. Weber, and J. Äystö, Phys. Rev. C **86**, 034337 (2012).

[44] J. K. Hwang, A. V. Ramayya, J. H. Hamilton, C. J. Beyer, X. Q. Zhang, J. O. Rasmussen, Y. X. Luo, S. C. Wu, T. N. Ginter, I. Y. Lee, C. M. Folden, P. Fallon, P. Zielinski, K. E. Gregorich, A. O. Macchiavelli, M. A. Stoyer, and S. J. Asztalos, Phys. Rev. C **65**, 054314 (2002).

[45] T. Rząca-Urban, M. Czerwiński, W. Urban, A. G. Smith, I. Ahmad, F. Nowacki, and K. Sieja, Phys. Rev. C **88**, 034302 (2013).

[46] J. Blachot, Nucl. Data Sheets **113**, 2391 (2012); Evaluated Nuclear Structure Data File, https://www.nndc.bnl.gov/ensdf/, 2009; S. Ohya, Nucl. Data Sheets **111**, 1619 (2010); J. Chen, *ibid.* **174**, 1 (2021).

[47] S. Eliseev, K. Blaum, M. Block, C. Droese, M. Goncharov, E. Minaya Ramirez, D. A. Nesterenko, Y. N. Novikov, and L. Schweikhard, Phys. Rev. Lett. **110**, 082501 (2013).

[48] D. Nesterenko, T. Eronen, A. Kankainen, L. Canete, A. Jokinen, I. D. Moore, H. Penttilä, S. Rinta-Antila, A. de Roubin, and M. Vilen, Eur. Phys. J. A **54**, 154 (2018).

[49] D. A. Nesterenko, A. Kankainen, J. Kostensalo, C. R. Nobs, A. M. Bruce, O. Beliuskina, L. Canete, T. Eronen, E. R. Gamba, S. Geldhof, R. de Groote, A. Jokinen, J. Kurpeta, I. D. Moore, L. Morrison, Z. Podolyák, I. Pohjalainen, S. Rinta-Antila, A. de Roubin, M. Rudigier, J. Suhonen, M. Vilén, V. Virtanen, and J. Äystö, Phys. Lett. B **808**, 135642 (2020).